POLITECNICO DI TORINO

Dipartimento di Automatica e Informatica

Master degree in Mechatronic Engineering

TESI DI LAUREA

DESIGN OF AN OMNIDIRECTIONAL GYROSCOPIC WAVE ENERGY CONVERTER

Relatori:

Prof.ssa Giuliana Mattiazzo

Ing. Giovanni Bracco

Candidato:

Fabio Carapellese

ANNO ACCADEMICO 2018/2019

It's just the beginning...

Contents

List of Figures

List of Tables

Introduction

The ISWEC, Inertial Sea Wave Energy Converter, is an offshore, single body, floating wave energy converter. The ISWEC research group so far has designed and developed a device where the floater consists of a monolithic steel hull with a semi-elliptical side profile, but rectangular from the up view. The actual ISWEC device is mono directional: for its correct functioning the hull needs to be aligned to the wave direction. The main objective of the thesis is to design an omnidirectional device capable to absorb energy from waves coming from any directions. This kind of configuration has been found to be optimal for the advantages introduced in terms of the WEC installation (no mooring system), as well as in terms of release time and finally improvement in safety. Such a device may be very useful to provide energy to small islands not connected to the national grid or to insulated marine system as for example fish farms. The main purpose of the thesis has been the design of the an omnidirectional ISWEC capable to produce 5-10kW. In particular, It has been done the dimensioning of the three main linked subsystems; the hull, the gyroscopic group and the Power Take Off (PTO) unit. The hull of the omnidirectional device is composed by a tin cylinder containing the gyroscopic group, the component responsible of the conversion of the mechanical energy into the electric energy, such as the electric generator and the electronic drives and the battery for the energy storage. For this new system the flywheel is mounted horizontally, and it is free to rotate with respect to its own axis. The gyroscopic effect is the result of the combination of the angular speed of the flywheel and the pith motion of the hull. The hull rotation happens about a reference axis that needs to be perpendicular to the flywheel direction. For the Inertial effect (Coriolis force) a torque is generated on the precession axis of the PTO that is rigidly connected to the gyroscope. To improve the hydrodynamic property of the system the cylinder needs to be coated with floaters, which are available commercially and are assembled

in polyethene modules filled with polyurethane foam. My studies have been focused on upgrading the mathematical model in order to understand better this new solution. The design involved the dimensioning of the gyroscopic group: its own mass inertia and the flywheel angular speed, the PTO selection, the optimization of the hull shape and then of its hydrodynamic property, and finally the design of the control parameters (the damping and the stiffness coefficient of the PTO shaft). Power losses plays a very important role in this kind of application, for this reason a design tool has been studied for selecting bearings which guarantee their work for 20 years and at the same time could minimize the power losses. For this preliminary study a linear model has been adopted to simulate the system on MATLAB. For the computation of the hydrodynamic characteristics of the system NEMOH approach has been used, which is an Open Source Boundary element method (BEM) code working on MATLAB.

Chapter 1

ISWEC:

Inertial wave energy converter

1.1 WEC introduction

Wave power has long been considered one of the most promising renewable anergies source. Ocean waves are a huge, but at the same time untapped energy resource, and the potential for extracting energy from wave is considerable. The use of waves as a source of renewable energy offers significant advantages over other method of energy generation :

- Sea waves offer the highest energy density among renewable energy sources. In particular, waves are more concentrated form of energy than wind: The wind velocity profile extends over several Km, consequently a wind farm explores a tiny sublayer, Instead, most of the wave energy flux is concentarted near the surface, then a wave farm can absorb a large part of the wave energy flux [1].

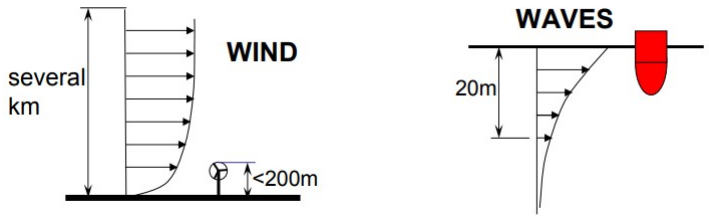

Figure 1.1: Velocity profile: comparison between wind and waves.

- Wave power devices can genereted power up to 90 percent of the time, compered to 20-30 per cent for wind and solar power device.

- Wave energy can provide utility scale power production. It also has application for remote island such as the Canary or Caibbean Island replacing expensive and polluting diesel power production. Furthermore, wave energy can power offshore industies such as fish farm, and oil and gas platform.

1.2 WEC classification

Despite the large variation in design and concepts, WECs can be classified into three predominant types[2].

- *Attenuator*: Attenuator lies parallel to the predominant wave direction and 'ride' the waves. An example of an attenuator WEC is the Palamis, developed by Ocean Power Delivery(now known as Palamis Wave Power). In figure 1.2a is shown an impression of a wave farm using Powerbuoys. The Palamis became the first offshore wave machine to generate electricity into the grid, when it was first connected to the UK grid in 2004.

  The Palamis is a floating device comprised of cylindrical hollow steel segments, having a diameter of 3.5 m connected to each other by two-degree-of-freedom hingeg joints. The central unit of each joint contains the complete power conversion system. The wave induced motion of the joints is resisted by four hydraulic cylinders that accomodate both horizontal and vertical motion. The cylinders acts as a pump, which drive fluid through a hydraulic motor, which in turn drive an electrical generator.

- $Point - absorber$: A point absorber is a device characterized by small dimensions with respect the incident wavelength. They can be floating structure that heave up and down on the surface of the water or submerged below the surface relaying on pressure differential. Because of their small size, wave direction is not relevant for this type of device. An example of point absorber is the Ocean Power Technology's Powerbuoy. As shown in Fig 1.2b OPT is a wave energy converter which is made up by three main component, the structure which is composed by the spar, a long

tube, and a heave plate. They do not move with the wave and they are stationary. The stucture hold on the top the floater which heave up and down exited by the wave. Then a Power take off system convert this heave motion into electricicty.

- *Terminator*: : terminator devices have their principal axis parallel to the wave front(perpendicular to the predominant wave direction) and phisically intercept waves. One example of a terminator-type WEC is the Salter's Duck, developed at the University of Edinburgh. The Duck concept is reported to be theoretically one of the most efficient devices. The Salter Duck is a system composed by a long spine to which is attached a *teardrop* shaped tool as ahown in Fig. 1.2c. Such tool faces the incoming waves and bobs as they pass. This bobbing action capture a massive amount of energy used to keep pistons running and then all the power take off system is actuated.

(a) Attenuator device: Palamis wave farm.

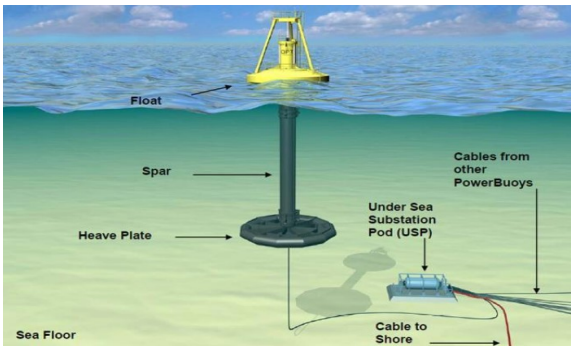

(b) Point absorber device: OPT Powerbuoy.

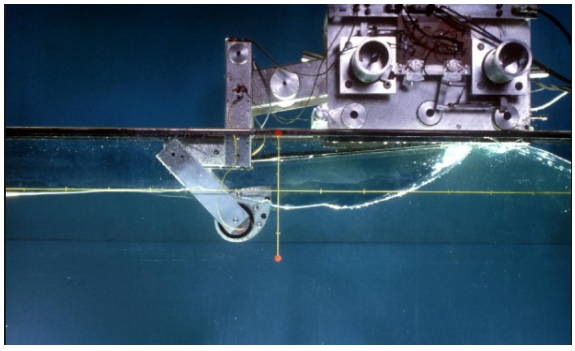

(c) Terminator device: Salter's Duck.

Figure 1.2: Examples of WEC devices.

Another straightforward method for classifying WECs is the deployment location.This classification gives information about availability, installation operational costs and the

kind of technology involved.

Onshore devices can be located at the shore and mounted above the see surface, integrated in civil infrastracture like a breakwater or a dam, fixed to a cliff. Advanteges are reduced installation and maintenance costs, given the easy accessibility and the lack of mooring system nor electric infrastructure. Disadvantages are that waves contain less energy and the high disruptive power of braking waves during storm.

Nearshore devices are installed in water from 10 to 25 meters, in moderate water deths. They can bee moored system or directly fixed to the seabed.

Offshore devices are located in deep water, with more than 40 meters of water deth. They are floaters or submerged structures moored to the seabed. Advantages are the higher power that they can access. On the other hand the distance from the coast makes the electric grid infrastructure installation and maintenance, very expensive.

1.3 ISWEC device

The ISWEC, Inertial sea wave energy converter, is a project studied and developed completely in the university framework at Politecnico di Torino, Department of Mechanical and Aerospace Engineering(DIMEAS). The idea was to exploit the gyroscopic effect created by the combined motion of the hull and the flywheel spinning speed for harvesting the wave energy and for converting it into electricity.

The ISWEC is defined as an offshore, single body, floating wave energy converter. A schematic representaion of the device is presented in Figure 1.3.

It consists of a monolithic hull, with an inner equipement room completely sealed with respect to the outer ocean environment. In the internal volume one or more gyroscopic units are installed. Also the electric PTO and the power conditioning system are completely enclosed into the floater. The only component that have continuity from the inside out is the electric cable, following the idea of a deploy plug device.

In normal energy production the device is alligned with the wave direction and the waves make the floater pitching around the δ axis. The floater pitch motion combined with the flywheel spinning velocity $\dot{\psi}$, generates an inertial gyroscopic torque acting on the internal precession axis ϵ.

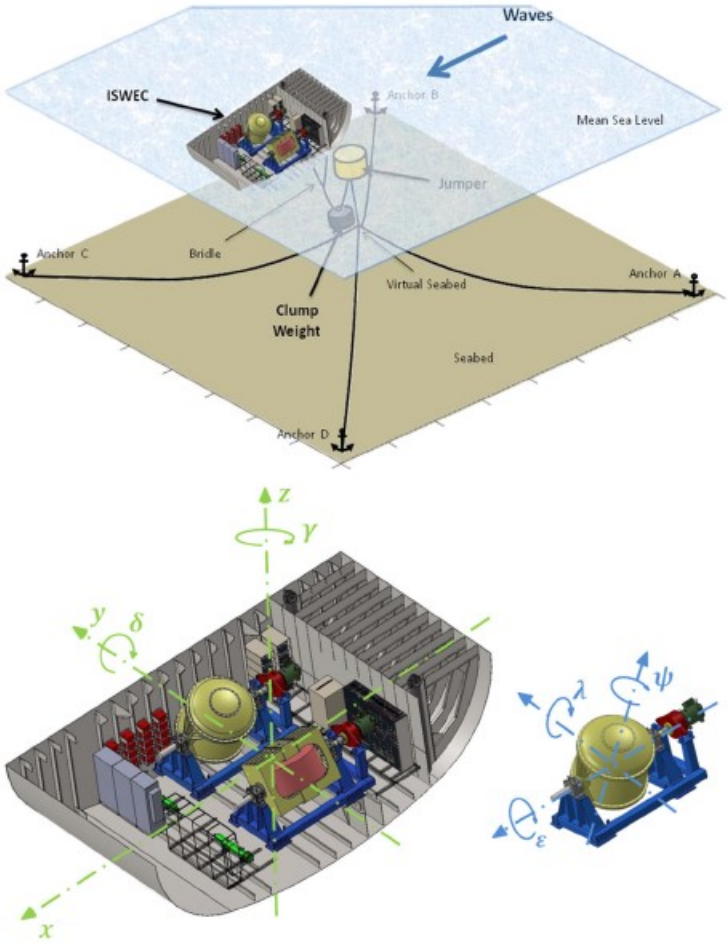

Figure 1.3: ISWEC prototype and installation drawings.

The exploitation of the gyroscopic effect anables the exchange of torque through the gyroscopic frame between the hull and the wave, providing the condition of power absorption. On the other hand, another fundamental feature of this technology is that the angular momentum responsable of the power conversion is dependent on the flywheel speed and then it can be easily tuned. In this way it is possible to actively change the natural resonant frequency of the system in accordance with the foreseen incoming wave climates.
Another important feature of the gyroscopic system power conversion is the transmission moltiplication that happens during the passage from the floater pitch oscillations(usually around 10 deg) to the oscillation of the internal gyroscope frame axis on which the PTO is mounted (about 60 deg).
Due to the gyroscopic working principle, the ISWEC is mainly conceived for working in the enclosed sea climates with reduced fetches, as the Mediterranean Sea, characterized

by waves with considerable steepness and high frequency.[7]

1.4 Glance to the future: Omnidirectional-ISWEC

Starting from the current design, a new hull shape is now created aming to maximize the device efficiency. The objective is to capture the wave power when its incident direction is not alligned to the x axis of the hull. As a first attempt in designing an omnidirectional ISWEC the geometric profile of the floater has been kept as simple as possible, providing that the final solid is axial-symmetric. Figure 1.4 shows an example of an omnidirection hull shape. It results that the values of the moment of inertia with respect x and y axes are conincident. Because of the new shape of the hull, the gyroscopic structure is mounted with the precession axis parallel to the hull axis of symmetry. A self-aligning mooring system is not required anymore. Having a revolutional hull entails, an updated analysis of the system is required and then it will be computed in the next chapters.

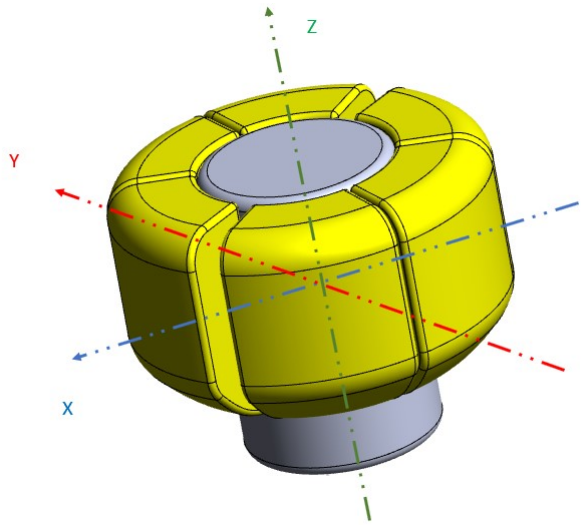

Figure 1.4: Example of an omnidirectional Hull Shape.

Chapter 2

Modelling

2.1 Introduction

This chapter has the role to introduce the modelling of the ISWEC system. It covers different phenomena involved in the power conversion (from the input wave to the electric power production). The theory behind the gyroscope system is analysed, together with the equations that characterized the beahaviour of an electric generator and the hydrodynamic interaction between the floater and the sea surface. This work has been already done in previous papers[7], but the aim of this chapter is to update the entire modelling for the $omnidirectional - ISWEC$.

2.2 Reference frames and definitions

In figure 2.1 some definitions about the reference frames are given. Also the three main components of the gyroscopic system are presented: the flywheel (green), the gyroscopic structure(brown) and the PTO(yellow).

- ECS: earth-fixed coordinate system(x_0,y_0,z_0)
- FCS: floater-fixed coordinate system(x_1,y_1,z_1)
- GCS: gyroscopic structure-fixed coordinate system(x_2,y_2,z_2)

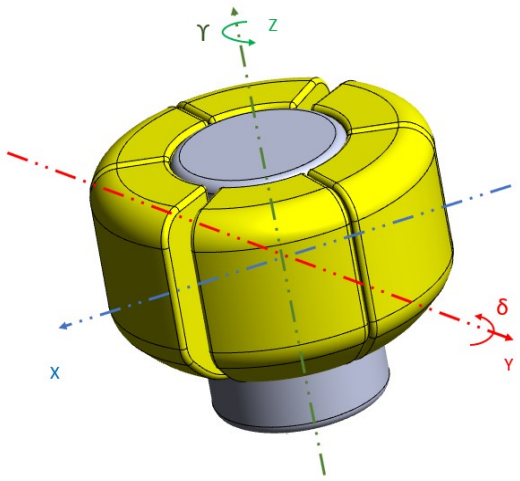

(a) Floater-fixed coordinate system

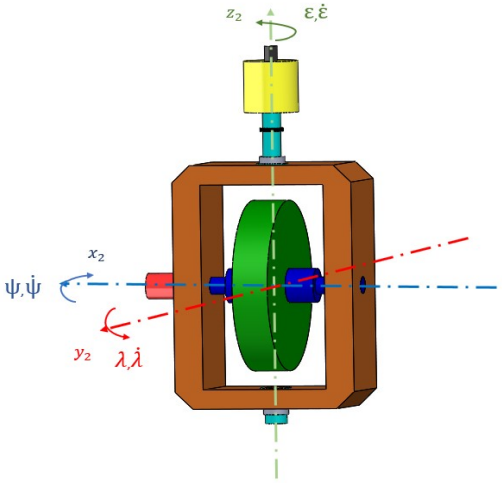

(b) Gyroscopic structure-fixed coordinate system.

As a first simplification, both the ECS and FCS origins are set in the center of gravity(CoG) of the system and x_1 is coincident with the wave direction, x_2 rotates with respect the precession axis.

DOF	Name	Comment	Symbol
1	surge	motion in the x_1-direction	x
2	sway	motion in the y_1-direction	y
3	heave	motion in the z_1-direction	z
4	roll	rotationsin about the x_1-axis	rx
5	pitch	rotationsin about the y_1-axis	ry,δ
6	yaw	rotationsin about the z_1-axis	rz,γ

Table 2.1: Hull-fixed FCS notations

DOF	Name	Comment	Symbol
1	-	-	-
2	-	-	-
3	-	$z_1//z_2$	-
4	-	rotationsin about the x_2-axis	ψ
5	-	rotationsin about the y_2-axis	λ
6	precession axis	rotationsin about the z_z-axis	ϵ

Table 2.2: Gyroscope-fixed GCS notations

As can be seen in Figure2.1, the FCS is the classical notations used for marine vehicles(Table 2.1). Once it has been considered a wave acting on the x_1 direction, the hull

rotations oround y_1 axis(δ) is called pitch and it is due to the wave floter-gyro interaction. In Table 2.2 GCS variables are also better defined. Of course not all the DOFs are free, since the gyroscope structure is fixed to the hull. The rotating PTO system is mounted on the precession ϵ-axis shaft. The flywheel is linked to the gyroscope structure with a revolute joint, so it's free to rotate around the x_2-axis with $\dot{\psi}$ speed.

2.3 Gyroscope system

The Gyroscopic system is the core of this technology and it represents the tool thanks with the kinetic energy of the floater can be turned in available mechanical energy on the internal precession axis. On the same internal shaft is mounted the PTO, which converts the mechanical energy into electricty.
There are mainly two ways to obtain the expression of the gyroscope dynamics: The Newtonian approach and the Lagrangian one. Of course both of them lead to the same results and in this section the Newtonian approach is computed.

2.3.1 Newtonian approach to the gyroscopic equations

Thus starting from the Newton's Second Law (*the change in momentum of a body is proportional to the force applied on it along the line on whitch the impulse is impressed*), the mechanical momentum generated on the CoG of the system by the angular momentum variation in time is evaluated. As known it is equal to the external generalized forces applied on the system:

$$\vec{M} = -\frac{d\vec{L}}{dt} = \sum_{i=0}^{N} \vec{T}_{E,i} \tag{2.1}$$

Note that the quantities involved are vectors. The absolute angular velocities of the GSA and the flywhhel respectively are written below:

$$\bar{\omega_2} = \dot{\psi}\vec{i_2} + \dot{\lambda}\vec{j_2} + \dot{\epsilon}\vec{k_2} \tag{2.2}$$

$$\bar{\omega_3} = (\dot{\phi} + \dot{\psi})\vec{i_2} + \dot{\lambda}\vec{j_2} + (\dot{\epsilon})\vec{k_2} \tag{2.3}$$

The GSA axes versors are $\vec{i_2}$, $\vec{j_2}$, $\vec{k_2}$ respectively for x_2, y_2,z_2. If such reference frame

is constitued by principal axis of Inertia, the tensor of the flywheel $\bar{I}_g$, may be written as follow:

$$\hat{I}_g = \begin{bmatrix} J & 0 & 0 \\ 0 & I_g & 0 \\ 0 & 0 & I_g \end{bmatrix}$$

Where J is the moment of Inertia around x-axis, while I_g is the moment of Inertia around the y and z axis. These values are constant in the GSA and the gyroscope angular momentum can be expressed as:

$$\bar{L} = \hat{I}_g \cdot \bar{\omega}_3 = J(\dot{\phi} + \dot{\psi})\vec{i}_2 + I_g\dot{\lambda}\vec{j}_2 + I_g\dot{\epsilon}\vec{k}_2 \tag{2.4}$$

Since its time derivative involves the versors derivation it has to be remembered that the time derivative of a versor is equal to the cross product of the angular speed of that versor by the same versor. In this case the generic angular spped of the GSA reference frame is $\bar{\omega}_2$ and the following exprssion can be written:

$$\frac{d\vec{i}_2}{dt} = \bar{\omega}_2 \wedge \vec{i}_2 = -\dot{\lambda}\vec{k}_2 + \dot{\epsilon}\vec{j}_2 \tag{2.5}$$

$$\frac{d\vec{j}_2}{dt} = \bar{\omega}_2 \wedge \vec{j}_2 = \dot{\psi}\vec{k}_2 - \dot{\epsilon}\vec{i}_2 \tag{2.6}$$

$$\frac{d\vec{k}_2}{dt} = \bar{\omega}_2 \wedge \vec{k}_2 = -\dot{\psi}\vec{j}_2 + \dot{\lambda}\vec{i}_2 \tag{2.7}$$

The dynamic equation of the gyroscope relates the external forces acting on the gyroscope to its angular momentum varation:

$$\bar{M}_e = J(\ddot{\phi}+\ddot{\psi})\vec{i}_2+J(\dot{\phi}+\dot{\psi})(\dot{\epsilon}\vec{j}_2-\dot{\lambda}\vec{k}_2)+I_g\ddot{\lambda}\vec{j}_2+I_g\dot{\lambda}(\dot{\psi}\vec{k}_2-\dot{\epsilon}\vec{i}_2)+I_g\ddot{\epsilon}\vec{k}_2+I_g\dot{\epsilon}(\dot{\lambda}\vec{i}_2-\dot{\psi}\vec{j}_2) \tag{2.8}$$

Its three scalar component in GSA are the following

$$\rightarrow \begin{cases} M_{x2} = J(\ddot{\phi} + \ddot{\psi}) \\ M_{y2} = I_g\ddot{\lambda} + J\dot{\phi}\dot{\epsilon} + (J - I_g)\dot{\psi}\dot{\epsilon} \\ M_{z2} = I_g\ddot{\epsilon} + J\dot{\phi}\dot{\lambda} + (I_g - J)\dot{\psi}\dot{\lambda} \end{cases} \tag{2.9}$$

In order to couple the hull model and the gyroscope model, it is usefull to write the gyroscope equation in LSA: the $\dot{\lambda}$ and $\dot{\psi}$ angular velocities are related to the pitch speed $\dot{\delta}$ as:

$$\dot{\lambda} = \dot{\delta} cos(\epsilon) \tag{2.10}$$

$$\dot{\epsilon} = \dot{\delta} sin(\epsilon) \tag{2.11}$$

Then the acceleration are equal to:

$$\ddot{\lambda} = \ddot{\delta} cos(\epsilon) - \dot{\delta}\dot{\epsilon} sin(\epsilon) \tag{2.12}$$

$$\ddot{\psi} = \ddot{\delta} sin(\epsilon) - \dot{\delta}\dot{\epsilon} cos(\epsilon) \tag{2.13}$$

Then equation (2.12),(2.13), (2,14) becames

$$\rightarrow \begin{cases} M_{x2} = J\ddot{\phi} - J\ddot{\delta} sin(\epsilon) - J\dot{\delta}\dot{\epsilon} cos(\epsilon) \\ M_{y2} = J\dot{\phi}\dot{\epsilon} + I_g\ddot{\delta} cos(\epsilon) - J\dot{\delta}\dot{\epsilon} sin(\epsilon) \\ M_{z2} = I_g\ddot{\epsilon} + J\dot{\phi}\dot{\delta} cos(\epsilon) + (J - I_g)\dot{\delta}^2 sin(\epsilon) cos(\epsilon) \end{cases} \tag{2.14}$$

Writing the equation in the hull reference frame

$$\rightarrow \begin{cases} M_{x1} = \bar{M}_e \cdot (\vec{i}_2 cos(\epsilon) - \vec{j}_2 sin(\epsilon)) = \bar{M}_{e,x_2} cos(\epsilon) - \bar{M}_{e,y_2} sin(\epsilon) \\ M_{y1} = \bar{M}_e \cdot (\vec{i}_2 sin(\epsilon) + \vec{j}_2 cos(\epsilon)) = \bar{M}_{e,x_2} sin(\epsilon) + \bar{M}_{e,y_2} cos(\epsilon) \\ M_{z1} = M_{z2} = I_g\ddot{\epsilon} + J\dot{\phi}\dot{\delta} cos(\epsilon) + (J - I_g)\dot{\delta}^2 sin(\epsilon) cos(\epsilon) \end{cases} \tag{2.15}$$

$$\rightarrow \begin{cases} M_{x1} = J\ddot{\phi} cos(\epsilon) - (J + I_g)\ddot{\delta} cos(\epsilon) sin(\epsilon) - J\dot{\phi}\dot{\epsilon} sin(\epsilon) + J\dot{\delta}\dot{\epsilon}(-cos(2\epsilon)) \\ M_{y1} = J\ddot{\phi} sin(\epsilon) + \ddot{\delta}(I_g cos^2(\epsilon) - J sin^2(\epsilon)) - 2J\dot{\delta}\dot{\epsilon} cos(\epsilon) sin(\epsilon) + J\dot{\phi}\dot{\epsilon} cos(\epsilon) \\ M_{z1} = M_{z2} = I_g\ddot{\epsilon} + J\dot{\phi}\dot{\delta} cos(\epsilon) + (J - I_g)\dot{\delta}^2 sin(\epsilon) cos(\epsilon) \end{cases} \tag{2.16}$$

Linearization The system (2.16) can be simplified considering small oscillation of the precession axis and then $sin\epsilon$ is considered equal to ϵ and the term $cos\epsilon$ equal to 1.

$$\rightarrow \begin{cases} M_{x2} = J\ddot{\phi} - J\dot{\delta}\dot{\epsilon}cos(\epsilon) \\ M_{y2} = I\ddot{\lambda} + J\dot{\phi}\dot{\epsilon} \\ M_{z2} = I\ddot{\epsilon} + J\dot{\phi}\dot{\lambda} \end{cases} \tag{2.17}$$

$$\rightarrow \begin{cases} M_{x1} = -J\dot{\phi}\dot{\epsilon}sin(\epsilon) \\ M_{y1} = I\ddot{\delta} + J\dot{\phi}\dot{\epsilon}cos(\epsilon) \\ M_{z1} = I\ddot{\epsilon} + J\dot{\phi}\dot{\delta}cos(\epsilon) \end{cases} \tag{2.18}$$

Variable due to the gyroscopic torque are :

$$\rightarrow \begin{cases} T_{\phi} = -J\dot{\epsilon}\dot{\delta}sin(\epsilon) \\ T_{\lambda} = J\dot{\phi}\dot{\epsilon} \\ T_{\epsilon} = J\dot{\phi}\dot{\delta} \end{cases} \tag{2.19}$$

2.4 Hydrodynamics

The interaction between hull and waves represents the very first stage in power conversion and a correct modelling of this phenomenon is fundamental for the description of the overall system behaviour. In general fluid dynamics phenomena are known to be difficult to be treated , both from an analytical and a numerical point of view, where computational power is still a limitation. Ideally the wave-body interaction could be studied solving the entire set of Navier-Stokes equations. Given that this equations can be solved analitically, the studied domain must be discretized and solved through numerical methods. Software packages able to carry out these evaluations are known as Computational Fluid Dynamics(CFD) codes. Even though it is possible to reach high fidelity results with this approach,its main limitations is related to the extremely high computation time required. Other compromise solution have been developed through years, having different trade-offs between modelling precision and required time. Linear, partially non-linear and non-

linear potential flow method have been widely studied and used in the field, being part of commercial and open-sofware suits. Linear potential flow codes enable the computation required in the fast-running Cummins lumped parameter equation. This method is at the basis of ISWEC hydrodynamic modelling.
In this section this low computational cost lumped parameters model used in the model-based design loop is introduced. It is a combination of already mentioned Cummis hydrodynamic linear integro-differential equation with a couples of viscous non linear terms and the contribution of some potential flow second order terms,as the mean drift forces.

2.4.1 Linear Cummis Equation

The equation describing the motion of the floater used in the model is trhe linear time-domain Cummins equation. This in considered tool for the modeling of the behaviour of a marine structure in waves. It is alinear time-invariant integrodifferential equation. The same equation can be written in frequency domain, with frequency dependand parameters. In the frequency domain it is easy to explore the main resonance properties of a floaters and having first draft designs.

Hyphothesis of the model The representation given by this model exploits the results of potential flow theories. Outcome of this theory is the pressure distribution around the floating body in steady-state condition, both at rest and exited by waves. This lead to the computation of the wave-floater exchanged forces and torques. In particular, Cummis deal with first order linear potential flow theory. Main hypothesis are:

- The fluid is incompressible;
- The fluid is inviscid;
- The fluid velocity field is irrotational. This means there are no vortexes;
- The body has zero or very slow forward motion;
- The body motion have small amplitude starting from the body equilibrium position, corresponding to a mean wetted surface.

The computation of the forces acting on the body can be splitted into differents terms. In the next paragraph they are detailed.

Time domain representation The first form here presented about the Cummins equation is in time-domain. It is an integro-differential equation with a convolution integral that described the fluid memory effects associeted with the radiation phenomena.

$$(M + A_\infty)\ddot{X} + \int_a^b h_r(t-\tau)\dot{X}d\tau + KX = F_w(t) + F_m(t) \tag{2.20}$$

This is a matrix equation, where $\vec{X}(\mathrm{j}\omega_n)$ vector contains the 6 DOFs of the floater: $X = [x, y, z, r_x, r_y, r_z]^T = [surge, sway, heave, roll, pitch, yaw]$. From the equation 2.20 is possible to distinguish the following hydrodynamic contribution:

- $KX(t)$: the hydrostatic restoring force. It represents the overall contribution of gravity and buoyancy forces on the floater in static.
- $A_\infty\ddot{X} + \int_a^b h_r(t-\tau)\dot{X}d\tau$: the radiation forces acting on the oscillating body in the fluid. Two effect are here evaluated:
  - $A_\infty\ddot{X}$:Added mass contribution. This term consider the acceleration of the fluid surrounding the hull.
  - $\int_a^b h_r(t-\tau)\dot{X}d\tau$: Radiation forces. This force is the damping force due to the waves generated by the hull motion. This is a dissipative effect and it is related to the velocity vector of the body.
- $F_w(t)$ is a force acting on the body exited by a monochromatic waves. In this case two effects are evaluated:
  - Froude-Krylov forces. These actions represent the waves forcing term for the whole dynamic equation. They are obtained by the integration over the hull submerged surface of the pressure fild generated by the undisturbed waves.
  - Difraction forces. The introduction of the floating body alters the wave surface, some waves are difracted. The pressure field is consequently influenced and then they are defined as the forces generated by the spatial integration over the floater wetted surface.

Instead, the term $F_m(t)$ is the dynamic exitation force acting on the mooring line which cosequently effects the dynamic of the floater.

Frequency domain representation The previous equation can also be defined in frequency-domain. It is a frequency-dependent coefficients, secon order, differential equation:

$$[-\omega^2[M + A_\infty)] + j\omega B(\omega) + K]X(\omega) = F_w(\omega) + F_m(\omega) \tag{2.21}$$

Where

- $\vec{X}(j\omega)$ is the vector which defines the floater 6-DOFS;
- M: floating body inertia matrix [6x6];
- A(ω): Frequency dependent added mass matrix [6x6];
- B(ω): Frequency dependent radiation matrix [6x6];
- K: Hydrostatic stiffness matrix [6x6];
- $F_w(\omega)$: Frequency dependant wave force vector [6x1];
- $F_m(\omega)$: Mooring line actions [6x1];

It must be noticed that coefficients are dependent either on the wave frequency and direction. The hypothesis in this analytic model is that the flywheel axis is aligned with the incoming wave front direction.

Difraction force modelling The translation of the radiation force between the frequency domain and time domain requires an accurate analysis. Th econversion of the Cummins' equation in frequency domain was computed by Ogilvie(1964) through the following relations:

$$A(\omega) = A_\infty - \frac{1}{\omega}\int_0^\infty h_r(t)sin(\omega t)dt \tag{2.22}$$

$$B(\omega) = \int_0^\infty h_r(t)cos(\omega t)dt \tag{2.23}$$

The impulse response function can therefore be written in time domain as:

$$h_r(t) = \frac{2}{\pi}\int_0^\infty [B(\omega) - B(\infty)]cos(\omega t)dt \tag{2.24}$$

and in the corresponding frequency response function:

$$Hr(j\omega) = B(\omega) + j\omega[A(\omega) - A_\infty] \tag{2.25}$$

The numerical comptutation of the the convolution term may be quite time-consuming and not well suited for the design and analysis of the wave enrgy converter. Perez(2008) suggested a smart way for overcoming this problem. For each element of the matrix h_r, since the covolution is a linear dynamic operator, the radiation force F_r can be converte in a linear ordinary differential equation.

2.5 3-DOF state space representation

For simplicity in the thesis work the device interaction with waves is reduced to a planar problem, with the work plane defined by the vertical gravity axis and the direction of the incoming wave. The planar approximation and the pitch only model, make the hydrodynamic linear [6x6] matrix problem to collapse into a scalar one, where the variable is the δ and its derivatives. The gyroscopic modelling also became a single differential equation governing the internal precession axis ϵ. At the end all the dynamic relationship can be reduced to system of one differential and one integro-differential equation given in eq.2.6: the first describes the dynamic behaviour of the internal precession axis and the second the floater pitch degree of freedom.

$$\begin{cases} T_\epsilon = I_g\ddot{\epsilon} + J\dot{\phi}\dot{\delta}cos\epsilon \\ \tau_w = (I_{eq} + \mu_\infty)\ddot{\delta} + \int_0^t \dot{\delta}(\tau)h(t-\tau)d\tau + \beta|\dot{\delta}|\dot{\delta} + K_w\delta - J\dot{\phi}\dot{\epsilon}cos\epsilon \end{cases} \tag{2.26}$$

In the first equation T_ϵ is the PTO torque, I_g is the overall momentum of inertia around the PTO ϵ-axis, J is the gyroscope axial momentum of Inertia, $\dot{\phi}$ is the flywheel velocity. In the second equation, τ_w represents the wave induced torque on the floater, I_{eq} is the

device momentum of inertia around the pitch DOF, μ_∞ is the istantaneous added mass and $\int_0^t \dot{\delta}(\tau)h(t-\tau)d\tau$ is the convolution integral representing the radiation force memory effects, having the impulse response in the Kernel, K_w is the linear hydrostatic stiffness and β is the quadratic viscous term. The gyroscopic effect owed to inertial momentum quantity $\mathrm{J}\dot{\phi}$ dinamically links the two equations with nonlinear coupling terms. It can be easily noticed that the two axis become independent when the flywheel velocity $\dot{\phi}$ equals to zero.

The last missing element is the description on the T_ϵ contribute. This the torque applied by the Power Take Off electric generator. In order to keep the flywheel axis oscillating around the vertical, the control low is design as follow:

$$T_{\epsilon PTO}(t) = -k\epsilon(t) - c\dot{\epsilon}(t) \tag{2.27}$$

It is made of a stiffness component proportional to the angular distance from the vertical ϵ, and a damping component proportinal to the same exis speed $\dot{\epsilon}$. A reactive power flux between the PTO and the sea surface is expected, due to the presence of the stiffness component.

2.5.1 State Space Pitch DOF linear model

Starting from the system of equation 2.26, the problem is hereafter reformulated in a state space form. A required step is to reformulate the convolution integral term μ, which can be reshaped in an approximated state space shape.

$$\mu = \int_0^t \dot{\delta}(\tau)h(t-\tau)\dot{\delta}d\tau \simeq \begin{cases} \dot{x} = A_{rad}x + B_{rad}\dot{\delta} \\ \mu = C_{rad}x \end{cases} \tag{2.28}$$

It is then possible to rewrite the overall system in a set of a first order linearized differencial equation,known as state space representation. The general form is the proposed:

$$\dot{X} = AX + Bu + B_d w \tag{2.29}$$

where X is the state vector containing the gyro frame positionand speed for modelling the precession axis dynamic, the pitch angle and its rate for describing the floater motion and n states required by the approximation of the wave radiation convolution integral.

$$X = [\dot{\epsilon}, \epsilon, \dot{\delta}, delta, \rho_{rv1}...\rho_{rvn}]^T \tag{2.30}$$

u in the controllable input. It is the PTO electric motor torque(T_{PTO}) after being multyplied by the gear ratio ($T_{\epsilon_{PTO}}$).
B is the controllable input matrix.

$$B = [\frac{1}{I_g}, 0, 0, 0, 0...0]^T \tag{2.31}$$

Instead, w is the uncontrollable unknown input. It is the wave disturbance. This is the torque exerted by the waves on the floater pitch degree of freedom.
$B : d$ is the wave disturbance input matrix.

$$B_d = [0, 0, \frac{1}{I_{eq} + \mu_{infty}}, 0, 0, ..0]^T \tag{2.32}$$

A is the system matrix. It is linearized around ϵ=0, that is for having the flywheel rotational axis inside the ISWEC longitudinal plane. For sake of simplicity the following substitution is made: $I_{eq} = I + \mu_{infty}$.

$$K_{ansys} = \begin{bmatrix} 0 & 0 & 0 & 0 & 0 & 0 & 0 & ... & 0 \\ 1 & 0 & 0 & 0 & 0 & 0 & 0 & ... & 0 \\ -\frac{J_g\dot{\phi}}{I_{eq}} & 0 & 0 & -\frac{K_w}{I_{eq}} & -\frac{c_1}{I_{eq}} & -\frac{c_2}{I_{eq}} & -\frac{c_3}{I_{eq}} & ... & -\frac{c_n}{I_{eq}} \\ 0 & 0 & 1 & 0 & a_1 & a_2 & a_3 & ... & a_n \\ 0 & 0 & 0 & 0 & 1 & 0 & 0 & ... & 0 \\ 0 & 0 & 0 & 0 & 0 & 1 & 0 & ... & 0 \\ \vdots & \vdots & \vdots & \vdots & \vdots & \vdots & \ddots & 0 & 0 \\ 0 & 0 & 0 & 0 & 0 & 0 & 0 & 1 & 0 \end{bmatrix}$$

The viscous term, can also be added, but in this design stage it is neglected. It is a measure of the fluid resistance to deformation at a given rate, then it works as a damper

for the float dynamic.

2.5.2 Control

The control strategy used in the design of the device and implemented in the IDT is the proportional derivative control, hereafter referred as "PD". It consists in the sum of two components: a part proportional to the precession angle ϵ starting from the zero vertical position and a part proportional to the speed $\dot{\epsilon}$ of the same axis.This control can be seen as a spring-damper control, where the first is the stiffness component and the second the damping action. In figure 2.1 the simple scheme of the torque set generation is shown.
The stiffness proportional part implies a reactive power flux. The absorbed active power is extracted by damping the rotation of the precession axis on which the gyroscopic frame is mounted. The damping action is needed for avoiding strong vibrations, but it has no effect on the final position of the PTO. The very few feedback measures required(PTO position and speed) and the simple architecture, make this system stable and robust, avoiding instabilities in case of highly irregular sea states. Even when the system is subjected to energetic sea states and the PTO goes into torque saturation frequently, the system remain stable. The linearity of PD control is extremely useful for being used in the pre-design phase, in the closed loop frequency domain analysis. In this domain it is possible to design and choose the parameters in order to set the internal mechanical system reconance frequency according to the incoming sea state spectra.
This control law drives the internal precession axis with a stable oscillating behaviour.

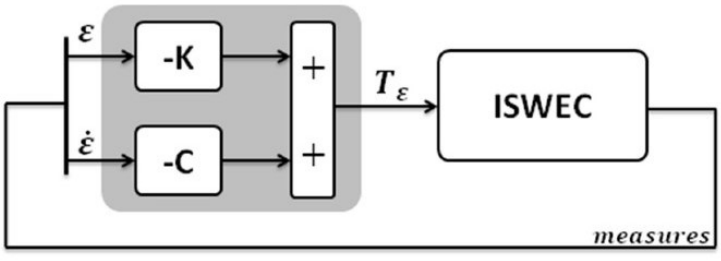

Figure 2.1: Control scheme.

Technicaltips

- The control parameters must keep the internal axis oscillations in a range of [40 60] deg in order to have higher enough speed on the internal precession axis for the power conversion and for staying in an area in which there is exchange of torque between the gyroscope system and the floater. In general for an oscillating control, the amplitude must be less then $90deg$ in order to have the gyroscopic torque agreeing with the floater motion.

- When the oscillation crosses the $\pm 180deg$, an offset of $\mp 180deg$ is summed to the feedback value, thus the value of the gyroscope frame angle ramains into the range [-180 180] deg.

Optimization and Tuning

This control is optimized offline, with the help of a numerical simulations. In particular, a set of three parameters are optimized for each sea state: the flywheel speed, the damping and the stiffness parameters. From a perspective of sensitivity on numerical modelling issues, if the model is not particulary good, the parameters are far to be optimal.

Chapter 3

ISWEC Design Tool

3.1 Introduction

In the previous chapter the linear model of the ISWEC system has been developed and studied. The best advantage of a linear model is his simplicity and computing velocity, really useful for a pre-design consideration. A set of functions has been developed in Matlab environment to satisfy this requirement. The main script allows the user to set and change all the design parameters of the system:

- Hull
- Gyroscope
- PTO
- Site of installation of the device

These will be the inputs of the algorithm. Once all the input parameters are defined, then an appropriete function builds the state space representations of the whole system. Then the software will optimize the PTO gross power for each wave of the scatter table, by choosing the most appropriate control parameters. The optimization is based on the cost function concept, in order to not overcome the system and simulation constraints, which can be modified by the user, and then the annual productivity can be calculated.

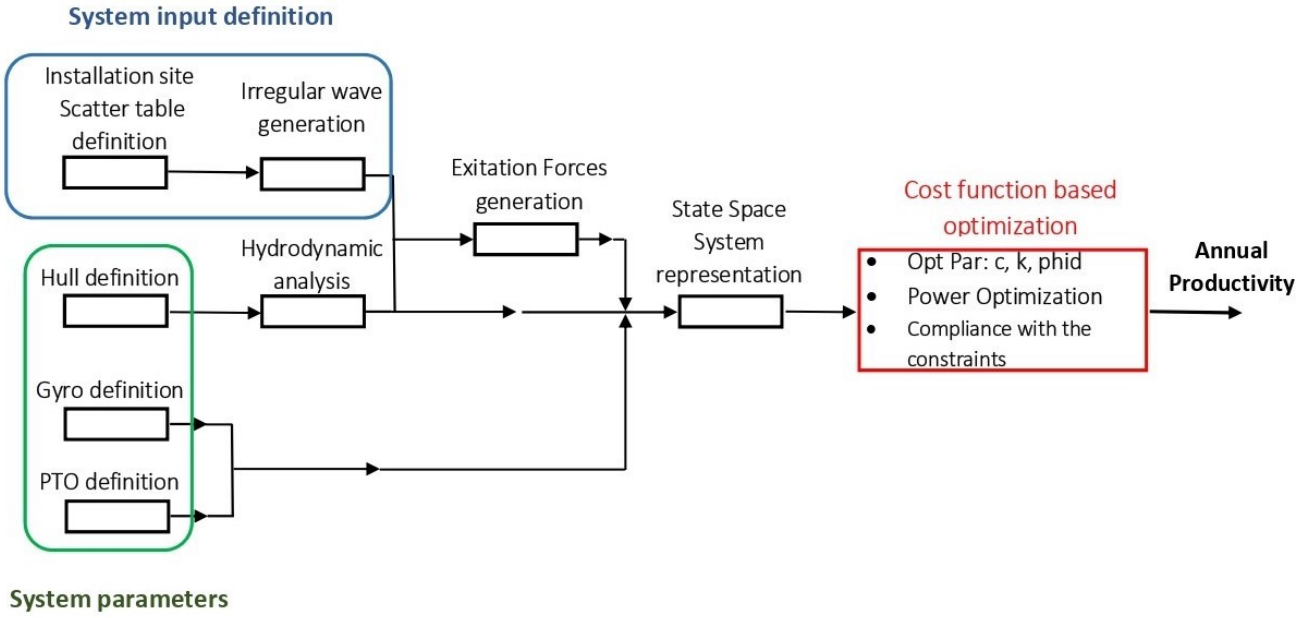

Figure 3.1: ISWEC design flow diagram.

3.2 System Parameters definition

The system parameters definition is the Matlab function that allows the user to choise the most important system characteristic and builds a parametric stucture suitable for the state space model representation. The system engineer can operate on these subsystem characteristics:

- Hull system
- Gyroscope system
- PTO system

In order to simplify the study of the system and make preliminary design considerations it is required to make some system assumptions. In a pre-design process it is necessary to constrain some variables, tying some parameters together with geometrical considerations or selecting some of them a priori, in order to reduce the number of free parameters on which to act for studying the system.

3.3 Hull definition

The hull definition is critical in this kind of application, its profile and shape has to be determined relating it to the installatuin site sea state in order to maximizing the exitation forces and the related displacement response. The algorithm allows to load the mass and the geometric properties of the floater. The geometric profile of the floater is set defining a picewice function which better approximate the choosen profile and then the 3-D geometry is built revoluting the profile with respect its axis of symmetry. In figure 3.1 is shown an example of the hull geometry definition. Once the hull has been defined its hydrodynamic properties are then computed:

- A(ω) Added Mass Matrix
- B(ω) Damping Matrix
- K(ω) Stiffness Matrix
- F(ω) Froude-Krilov and difraction forces

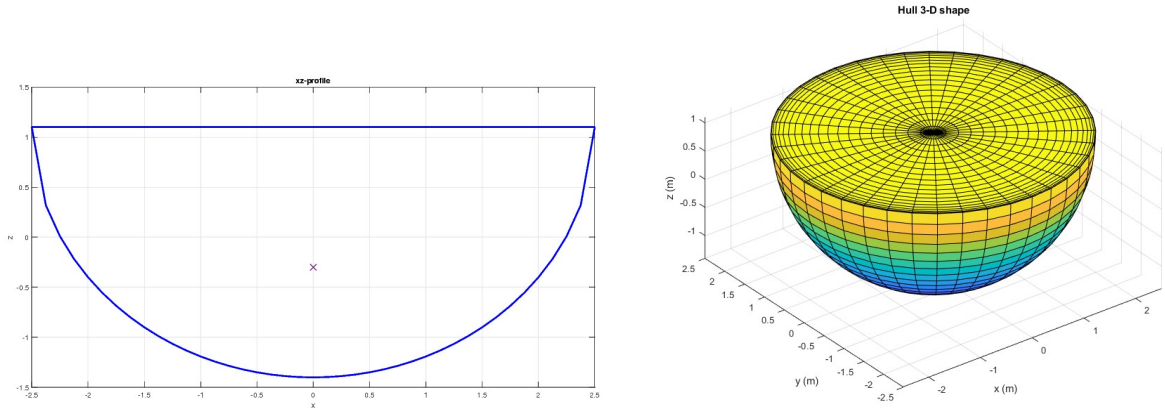

(a) hull **(b)** *complete system*

Figure 3.2: Hull geometry definition on Matlab.

These hydrodynamic properties are computed using NEMOH approach. It is an open source Boundary element Methods (BEM) code developed by resercher at Ecole Centrale de Nantes. A matlab wrapper NEMOH.m is provided and then it is easy to use NEMOH from the Matlab environment. The user is then required to given as input the hull surface and the mesh is genereted through the Matlab function axiMesh.m, provided by Nemoh. More precisely, the input parameters required by axiMesh.m are:

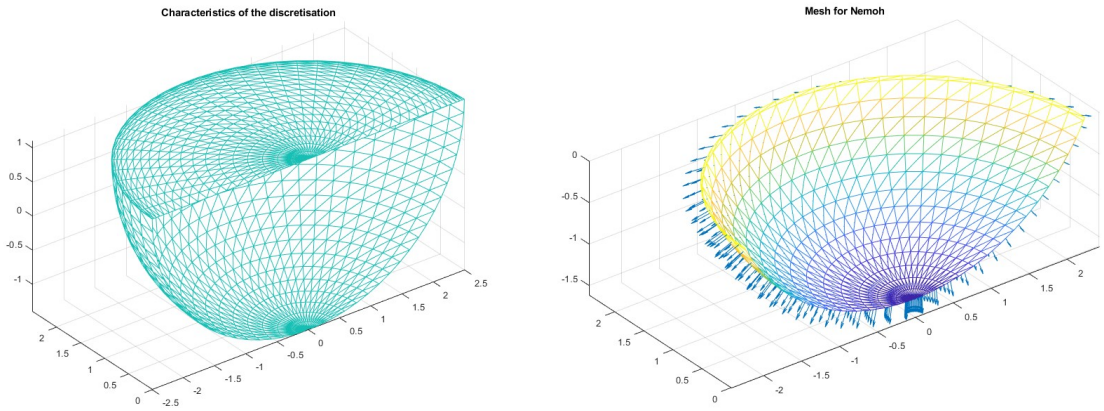

(a) hull **(b)** *complete system*

Figure 3.3: Meshing operation for Nemoh-half hull geometry.

- n : number of point for discretisation
- r : arrey of radial coordinates
- z : arrey of vertical coordinates

The outputs of such meshing step are shown in Figure 3.2. The outputs of the meshing operation are the coordinates of the Buoyancy center, and the hydrostatic stiffness matrix. Once the mesh as been computed, it is ready to be used by NEMOH processor which can than computed the hydrodynamic parameters listed at the beginning of the paragraph.

3.3.1 Perez Analysis

The hydrodynamic parameters computed by Nemoh are in frequency domain and and for discrete frequency values, then the Perez analysis is computed . It is a manual algorithm divided in two part: the first part tries to find the current order of transfer function that well approximates the added mass and radiation damping and the second one intervenes if the automatic procedure do not succeeded and ask the user to manually set the order of the curves which better fits the Nemoh.m results. To avoid the second part of the code, a new criteria is used: a root mean square error(RMSE) method is applied and the order that minimizes it is chosen. From past experiences, the most frequent orders are from 2 to 6 and, in order to reduce the running time, these are the extremes used in the analysis.

3.4 Gyroscope and PTO definition

The user has the possibility to load a specific gyroscope group, with a defined mass matrix and geometry properties or, through some assumptions, can set some variables of the flywheel, and the algorithm compute the mass matrix.

The gyroscpe is the main system in the energy conversion process. It is the core of this technology and it represents the intermediate stage between the sea wave power and the electric power available for the user. The gyroscope system includes the flywhhel, the support frame, and the bearings. The Flywheel is the most important system element regarding the energy conversion. The exchange of generalized forces with gyro-frame, hull and the waves is strongly related with its moment of inertia. The bearings have to support either the gyroscopic torques and the flywheel weight. The choosen solution is the configuration with only two radial bearings capable to bear the weight of the flywhhel too. Figure 3.3 shows the gyroscope geometric parameters that are considered in this work.

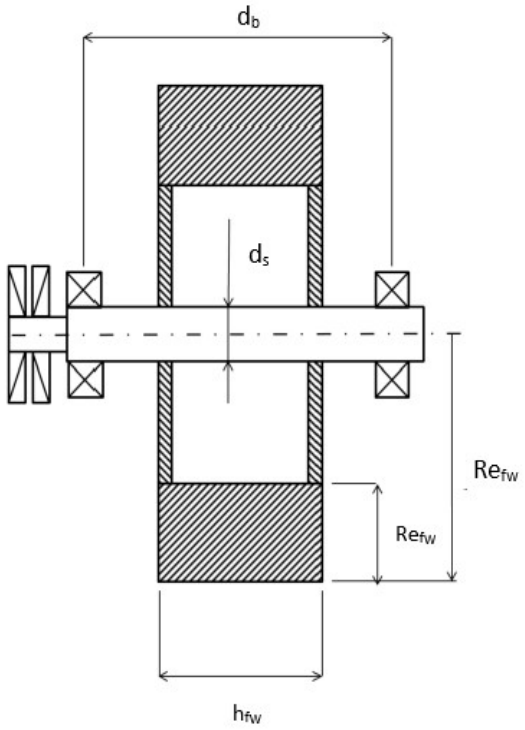

Figure 3.4: Flywheel section and quotes

The gyroscope is geometrically defined by the following parameters:

- h_{fw} is the flywheel axial height
- R_e is the flywheel outer radius
- R_i : is the flywheel inner radius

Due to the symmetry of the geometry the inertia tensor is diagonal:

$$\bar{I_{fw}} = \begin{bmatrix} J & 0 & 0 \\ 0 & I_{yy} & 0 \\ 0 & 0 & I_{xx} \end{bmatrix}$$

The flywheel can rotate about its axis of symmetry through an electric motor and its speed can be regulated considering the see states.The flywheel is connected to the support frame through two radial bearings mounted on its shaft. Other two thrust bearings allow the connection between the support frame and the structure fixed to the hull. The precession oscillation of the gyroscope can be transformed into electricicty by a suitable Power Take Off system.
To the gyroscope is connected the PTO subsystem. For the purpose of the analysis performed in this final work the dynamic of the elctric drive is neglected, and it it modelled as an ideal linear relationship. A gearbox is installed between the electric motor and the gyro frame shaft. For semplicity at this stage the gear-ratio is set to one, then the resulting torque on the flywheel shaft will affect directly the electric generator. The main parameters regarding the electric generator are:

- Nominal Torque T_{nom}
- Maximum Torque T_{max}
- Nominal speed ω_{nom}

3.5 System input definition

One of the most important quantity to take into account during the first dimensioning of the wave energy system is the annual productivity, and the main objactive is to maximize

it. Each ISWEC device configuration depends on the representaive see state scatter table that better represents the sea where the device is going to be instal.

3.5.1 Scatter table

The wave represenation is the primary energy of this application, then the devide is required to capture and transform into electric energy as much energy as possible. The wave is the input of such system and its interaction with the hull generets the exiting forces of the sytem. To evaluete the real potential of the device in longer term, at least yearly data are required. For the pre-design of the omnidirctional ISWEC the Pantelleria Scatter table is taken as a reference. It is an important tool that describe the hours of occurence of a specific wave in one year; each wave is represented by a significant height and by an energy period. Here below is represented the Pantelleria Scatter Table reporting data recorded in 2010. Observing the occurence scatter table it is possible to notice that

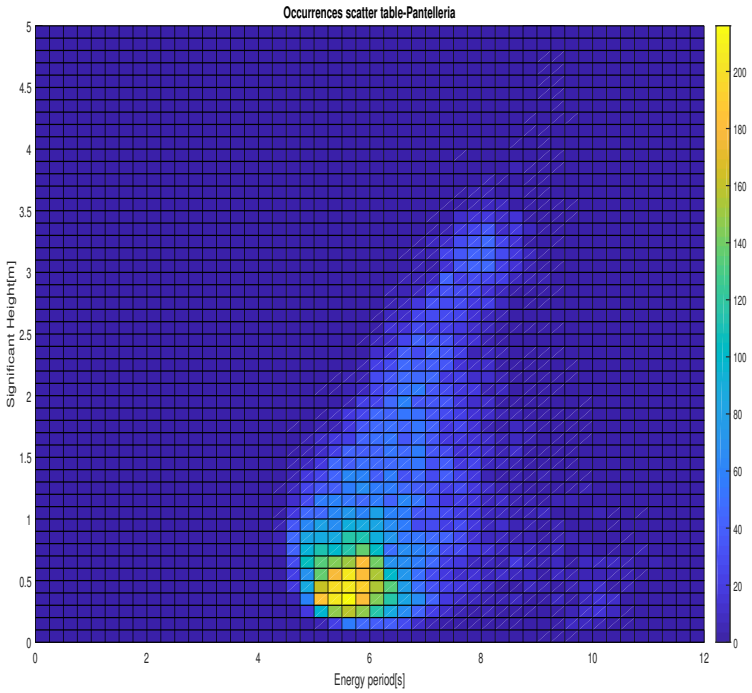

Figure 3.5: Pantelleria sea-state Occurrences Scatter Table.

the most occurent sea state is about H_s equal to $0.5m$ and T_e equal to $5.75s$

3.5.2 Model of the wave

For its nature, a wave cannot be reduced to a simple periodic pattern And cannot be defined in a closely deterministic way, then the term random vibration is commonly used to define this kind of forcing function. In figure an example of a simulated wave is shown. Then irregular wave can be seen as the summation of N single regular waves:

$$\eta(t) = \sum_{i=1}^{N} \frac{H_i}{2} sin(2\pi f_i t + \phi_i) \tag{3.1}$$

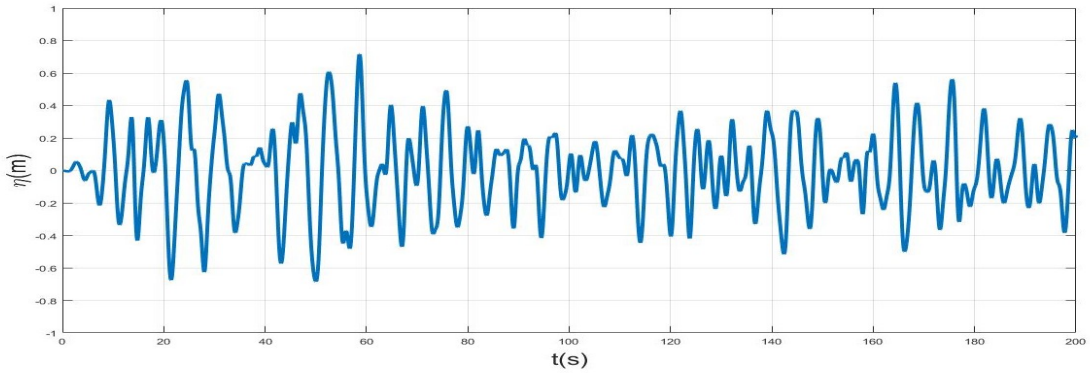

Figure 3.6: Wave representation-Time series

In random sea theory the phase ϕ_i is arbitrary or random and it is uniformly distributed on [0;2π]. They can be described through a frequency domain representation. The distribution of the wave elevation as a function of the frequencies is normally defined as a wave spectrum. Thus a wave profile time history can be studied and defined using some scalar indexes, in particular starting from the so-called moment of distibution. In general, $n-th$ order moment for a finite intervals of frequencies is approximated in the following way:

$$m_n = \sum_{i=0}^{N} f_i^n \frac{a_i^2}{2} \tag{3.2}$$

where a_i^2 represents the variance contained in the defined $i-th$ interval δf.
As mentioned the key parameterms for defining a specific sea state are:

- **Significant wave height**. This value is defined as the average of the highest one-third of the wave heights. It is possible to carefully estimate it also starting from

the zero order momentum of the wave distribution.

$$H_{m_0} = 4\sqrt{m_0} \tag{3.3}$$

where m_0 is the total variance of the wave record obtained by the sum of the variances of the individual spectral component.

- **Wave energy period**. This parameter gives information about the energetic content of the analysed irregular wave. It is calculated using the following relationship:

$$T_e = \frac{m_1}{m_0} \tag{3.4}$$

From these parameters the computation of the energy content of a wave, its power density can be specified:

$$J_{irreg} = 0.49 H_s^2 T_e \tag{3.5}$$

Where J is the power density in kW/m, H_s is the significant wave height in m and T_e is the wave energy period in s

The significant wave height and wave period are fundamental for having an estimation of the entire wave spectrum of the Pantelleria sea states. From these parameters the wave time series is genereted using the WAFO.m tool on Matlab which using the $JONSPAP$(Joint North Sea Wave Project) spectrum simulates a wall specific wave. The general form of such distribution function is shown in the following figure.

The function which describes the power density distribution of the JONSWAP distribution is:

$$S(f) = \frac{\alpha g^2}{(2\pi)^2 f^5} e^{-1.25(\frac{f}{f_p})^4} \gamma(f) \tag{3.6}$$

Where f is the wave frequency, g is the acceleration due to gravity(m/s^2) and α is a dimensionless quantity, empirically determined, equal to 0.0081. The function γ is the peak enhancement factor, which modify the interval around the spectral peak and makes it different from the Pierson-Moskowitz spectrum[2].

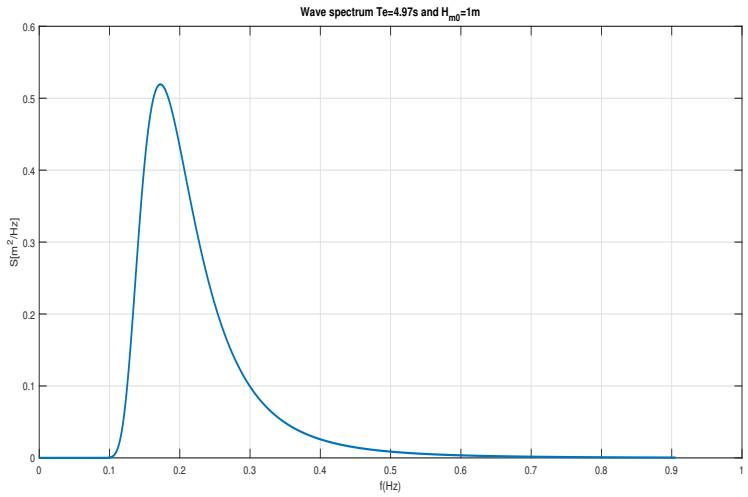

Figure 3.7: General form of a JONSWAP spectrum as a function of f

3.6 Cost function

Starting from the state space model and input, that could be a regular wave, recorded irregular wave or pseudo random irregular wave, a new optimization algorithm has been developed, based on the cost function concept, that take into account any system constraints. The main objective of the optimization algorithm is to maximize the PTO net power production, acting on the system parameter c,k,$\dot{\varphi}$, while taking care to do not overcome the system constraints. This can be reached introducing a cost function J.
A cost function is a function that maps the values of some variable onto a real number, intuitivly representing some "cost" associeted with the event. An optimization problem seeks to minimize the cost function. The cost function J consists mainly of two parts, the net mean power term and the system constraints term.

$$J = P^*_{net_{mean}} + \Sigma J_i \tag{3.7}$$

The power term is a negative real number, instead the cost of the constraints is the sum of all the contributes related to the constraints which are positive numbers. In order to have contributes of the same magnitude, both power terms and constraints are normalized with respect the maximum term reachable. The cost functions terms are hereafter shown.

Each of them refer to a dimensionless variable:

$$P^*_{net_{mean}} = \frac{P_{net_{mean}}}{P_{nom_{PTO}}} \tag{3.8}$$

$P^*_{net_{mean}}$ is the net power mean, the term that must be minimized: in agreement with the power sign convention the genereted power is negative. $P^*_{net_{PTO}}$ is the retad power of the PTO.

$$\epsilon^*_{max} = \frac{\epsilon_{max}}{\epsilon_{max_{constr}}} \tag{3.9}$$

$$\epsilon^*_{rms} = \frac{\epsilon_{rms}}{\epsilon_{max_{constr}}} \tag{3.10}$$

It is appropriate to consider both the *rms* and the constraint on the maximum value because of the irregularity of the input signal which represents the wave. $\epsilon_{rms_{constr}}$ and $\epsilon_{max_{constr}}$ are respectively the constraits on the root mean square and maximum value of the internal PTO axis angle, the former is set to avoid an undesired working regime, the latter is a matter of stability.

$$\delta^*_{max} = \frac{\delta_{max}}{\delta_{max_{constr}}} \tag{3.11}$$

$$\delta^*_{rms} = \frac{\delta_{rms}}{\delta_{max_{constr}}} \tag{3.12}$$

$\epsilon_{rms_{constr}}$ and $\epsilon_{max_{constr}}$ are respectively the constraits on the rms and maximum value of the hull's pitch angle, in order to guarantee that the Cummis equation remains valid.

$$T^*_{PTOmax} = \frac{T_{PTO_{max}}}{T_{PTOmax_{constr}}} \tag{3.13}$$

$$T^*_{PTOrms} = \frac{T_{PTO_{rms}}}{T_{PTOmax_{nom}}} \tag{3.14}$$

$\epsilon_{rms_{constr}}$ and $\epsilon_{max_{constr}}$ are respectively the constraits on the rms and maximum value of the PTO torque. It is recommended to not overcome the nominal PTO torque otherwise the thermic regime of the PTO exceed the technical specification of the machine.

$$\omega^*_{PTOmax} = \frac{\omega_{PTO_{max}}}{\omega_{PTO_{nom}}} \tag{3.15}$$

The $\omega_{PTO_{nom}}$ is the PTO speed and it is necessary to not exceed this value, otherwise the electric voltage at the inverter overcome the technical specifications of the machine and

the inverter.

After having presented all the normalized terms, the cost functions for each constraint is now presented. Calling x^* a generic constraint dimensionless term, the cost related to it is defined by the equation:

$$J(x^*) = \frac{1 + tanh100(x^* - 1)}{2} + H(x^*) \cdot (x^* - 1)^2 \tag{3.16}$$

Where $H(x^*)$ is the Heaviside function so defined:

$$H(x) = \begin{cases} 0, \ x^* < 1 \\ 1, \ x^* > 1 \end{cases} \tag{3.17}$$

3.7 Optimization algorithm

A constrained optimization is defined by the minimization of the object function. This process happens under a certain number of constraints: it is required to minimize the object function $F(X)$ searching the *optimized* value x_i which can be choosen insisde predefined interval, considering a given set of constraints g_i. The vector X of the design parameters to optimize is here defined:

$$x = [c, k, \dot{\varphi}] \tag{3.18}$$

The optimization algorithm chosen is a Global Optimization Algorithm. These algorithm search for global solution to problem that contain multiple maxima or minima. In particular the $ParticleSwarm$ optimization method has been used for the purpose of the the ISWEC tool. It is a computational method that optimizes a problem by iteratively trying to improve a candidate solution with regard to a given measure of quality. It solves a problem by having a population of candidates solution, here defined particles, and moving these particles around in the search-space according to simple mathematical formulae over the particle's position and velocity. PSO is a metaheuristic method as it makes few or no assumption about the problem being optimize and can search very large space of candidates solution.

A global optimization algorithm guarantees a better result in term of the minimization

of the cost function with respect a local optimization algorirhm , which finds the minimum of a scalar function studying the possible solution around a starting set of variables. Being a global optimization method it is more time consuming the a local optimization algorithm, but PSO has been evalueted in previous workd as the fastest method about computation time with respect other global optimization algorithm.
Considering the objective of designing a decice able to produce up to $10kW$ of power, here below are reported for each design parameter the interval of definition:

$$0 \leq \dot{\varphi} \leq 1700 \text{ (rpm)}$$

$$0 \leq c \leq 10^5 \text{ (Nms/rad)}$$

$$0 \leq k \leq 10^5 \text{ (Nms/rad)}$$

The PTO system choosen for the size of this application has the following characteristic

Quantity	Unit	Value
max PTO power	[kW]	85,50
max PTO Torque	[Nm]	5700
nom PTO Torque	[Nm]	3500
max PTO angular speed	[rpm]	1500
Gear ratio		1

Table 3.1: PTO parameters.

The constraints related to the dynamic responses of the device are hereafter reported

Quantity	Unit	Value
ϵ max	[deg]	150
ϵ rms	[deg]	70
δ max	[deg]	50
δ rms	[deg]	20
ϕ max	[rpm]	1700
T_{PTO} max	[Nm]	5700
T_{PTO} rms	[Nm]	3500

Table 3.2: Simulation constraits.

Chapter 4

Omnidirectional ISWEC design

4.1 Introduction

A wave energy converter is a mechatronic system able to exploit the wave power and to convert it into evergy. The fuctioning of the ISWEC device is determined by the right interaction between the floater body, the gyroscopic group ,and the Power Take Off(PTO) unit. For the design of a small size device (from 3 to 5 kW) the experience in this application of the ISWEC team and Wave for Energy S.r.l. engineers has been very important. Objective of this chapter is to present a preliminary design of an omnidirectional gyroscopic WEC. The results in terms of produced net power are shown through the simulation of the system on Matlab using a linearized 3-DOF model.

4.2 The ISWEC-Omnidirectional configuration

The objective of the floater of an ISWEC device is to maximaze the pitch response in the range of frequencies characteristic of the installation site. The system overall response can be regulated through the control of the characteristic parameters of the gyroscopic group.

The first step in an ISWEC design is the geometry identification, which has to be easy to parametrize and flexible as much as possible. The first profile shape taken as refence is the Pantelleria device profile. A sketch of the shape(red line), with the relative quantities in shown in figure 4.1. This geometry is axially symmetric and thus it can be evaluated

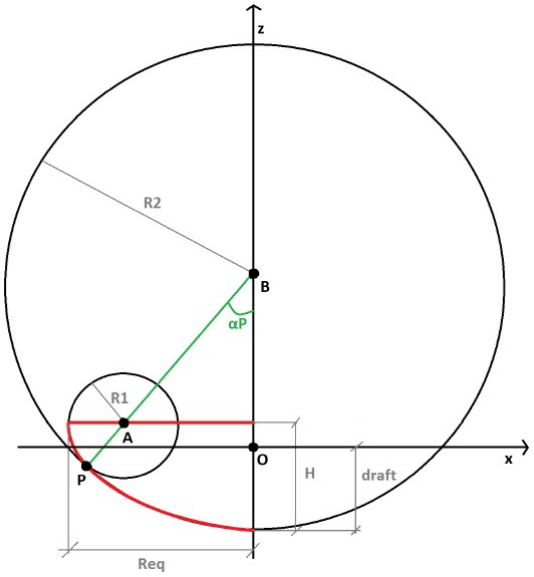

Figure 4.1: Sketch of the profile shape of the floater.

just the part of the profile that will be revoluted. In this case XZ-plane is chosen, where the x-axis is coincident with the water level and the z-axis is on the vertical direction. The parameters involved in this geometrical solution are:

- **draft**: distance between the water level and the lowest point on vassel(LPV);
- **R1 and** x_A: radius and x-coordinate of the circle C1 (z-coordinate is fixed and equal to z_{aff});
- **R2 and** z_B: radius and x-coordinate of the circle C2 (z-coordinate is fixed and equal to zero);
- R_{eq}: hull equivalent radius (Req=R1+x_A)
- **H**: hull height

It has been demonstrated that such geometry gives good results in term of device annual productivity, all the detailed results are presented in the following analysis. It is then an optimal solution in terms of hydrodynamic performance and resulting productivity, but for the actual realization of an omnidirectional device, such a hull shape may be quite complicated to manufacture or at least highly expensive. For a starting design of the device a different approach was then used, then as shown in figure 4.2 all the component

for the power conversion has been installed in a tin steel cylinder. The first step has been the dimensioning, in term of size, of all the functional component. Here below are summarized all the principal component:

- Gyroscopic structure
- PTO
- electric system
  - Batteries
  - Ultracapacitors
  - Power electronic and coverters

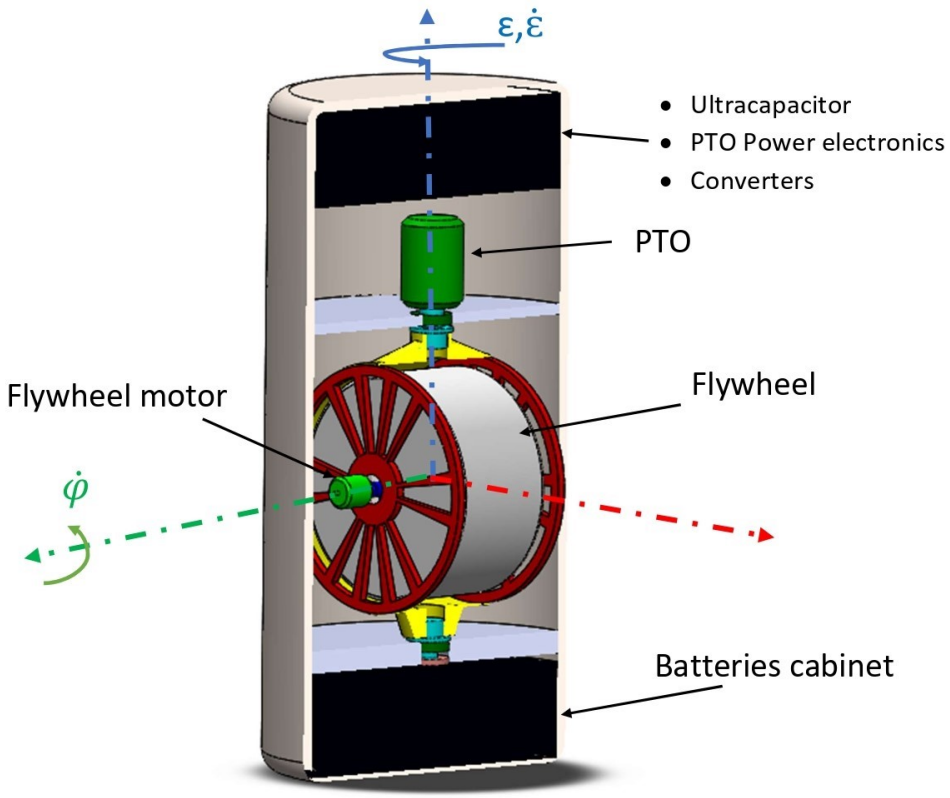

Figure 4.2: Schematic representation of the machine room configuration.

4.3 The gyroscope

The gyroscopic group is the key subsystem enabling the power conversion. The main specification of thr gyroscopic unit is the angular momentum. This is equal to the product of the flywheel axial momentum and its spinning velocity. Given the high inertial torque that have to be exchanged, component are required to have a noticeable size and heavy load duty conditions. A 3-D model of the gyroscope has been done in order to evaluate the weight of all the structure. A schematic representation of the whole gyroscopic group is shown in figure 4.3. The gyroscope frame is mounted on a shaft which is connected with the PTO by a gearbox.

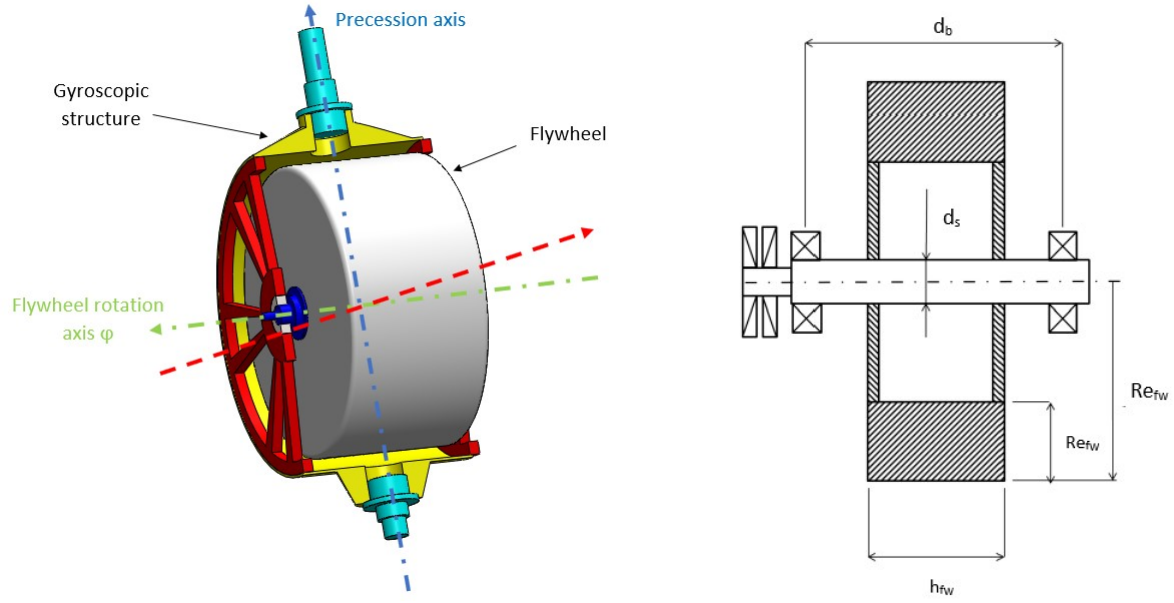

(a) *Gyroscopic unit: 3-D model.* **(b)** *Flywheel schematic representation*

Figure 4.3: Gyroscopic system representation.

The gyroscope geometry is a fundamental characteristic for the device power extraction.It is composed by a central element called crown and two short shafts section on both sides. The crown is made of an external cylindrical element that is strengthen by two side plates. This configuration has been adopted beacuse it guarantees a stiffer structure. The material considered for the ring is the S355 steel and the 39NiCrMo3 for both the semi-shaft. A schematic 3-D model on solidworks has been scketched and the resulting mechanical and geometrical properties of the gyroscopic unit are reported in Table 4.1.

The unit is provided of a vaccum chamber, a sealed case with a low pressure internal

Properties group	Quantity	Unit	Value
Geometry	Ring external diameter ($R_{e_{fw}}$)	[mm]	550
	Ring height(h_{fw})	[mm]	550
	Ring thickness (S_{fw})	[mm]	80
	Bearing distance(d_b)	[mm]	670
Mass properties	Mass	[kg]	2310
	Momentum of Inertia about axial rotational axis x	[kg m^2]	414.140
	Momentum of Inertia about transversal axis y	[kg m^2]	279.942
	Momentum of Inertia about vertical axis z	[kg m^2]	279.942

Table 4.1: Flywheel properties

environment. This is intended in order to reduce the aerodynamic losses of a rotating body. Then the flywhhel and the DC-motor connected to the flywheel rotational axis are enclosed in a frame. Such a frame is mounted on the PTO internal shaft and it is supported directly by the tin cylinder inner surface . The frame can rotate only about the internal precession axis z. Hereafter is reported the Inertia matrix of the support frame I_{fs}:

$$Ifs = \begin{bmatrix} 160 & 0 & 0 \\ 0 & 202 & 0 \\ 0 & 0 & 205 \end{bmatrix}$$

4.3.1 Flywheel motor

The component which makes the flywheel to rotate is an electric brushless torque motor made by Siemens, belonging to the SIMOTICS T-1FW3 family with high speed winding configuration.

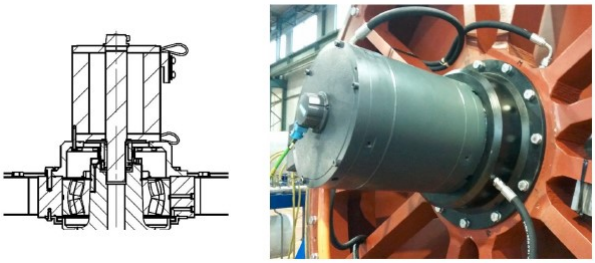

Figure 4.4: Flywheel motor.

Properties group	Quantity	Unit	Value
Mechanics	Rated speed	[rpm]	1200
	Rated Torque	[Nm]	970
	Maximum Torque	[Nm]	1700
	Maximum speed	[rpm]	1800
Electrics	Rated current	[A]	245
	Rated Voltage	[V]	480
	Rated Power	[kW]	117.5
	Maximum Current	[A]	3.2
Geometry	Main body longitudinal length	[mm]	338
	External diameter	[mm]	310
Mass	Mass	[Kg]	143
	Momentum of Inertia of the rotor	[Kgm_2]	0.13

Table 4.2: Flywheel motor, SIEMENS 1FW3154-1BP.

This electric machine is coupled with Siemens power electronic hardware, making possible the rotating speed regulation of the flywheel. The key technical information about the motor are shown in Table 4.2. A picture of the flywhell motor is shown in Figure 4.4. The rotation is allowed by a couple of radial spherical roller bearing which task is to support all the flywheel structure, in particular they take up the radial load due to the gyroscopic inertial torques and the flywheel own weight. These are the most stressed components in the system and usually their working life provides the time of the first return of the device in port. Details about bearings selection are presented in the next chapter.

4.3.2 The PTO

The Power Take Off system is completely electric. An electric generator directly affects the oscillation of the gyroscopic frame. It is mounted on the precession axis, along the z direction of the floater. High torques and low speed are common in wave energy field. Resulting torque for this kind of device can achive the value of 3kNm and a maximum speed of 20 rpm. The generator used as a reference has been choosen in order to avoid any gear reduction.

As shown in Figure 4.5 permanent Magnet Synchronus Torque Mootor is choosen as a

generator. It is supplied by SIEMENS, in particular it belongs to the SIMOTIC SERIES AND 1FW3 family. In table 4.3 the properties of the generator taken as a reference for the optimization analysis are presented.

Properties group	Quantity	Unit	Value
Mechanics	Rated speed	[rpm]	150
	Rated Torque	[Nm]	3500
	Maximum Torque	[Nm]	5700
	Maximum speed	[rpm]	1800
Electrics	Rated current	[A]	115
	Rated Power	[kW]	55
	Maximum Current	[A]	203
Geometry	Main body longitudinal length	[mm]	763.5
	External diameter	[mm]	540
Mass	Mass	[Kg]	1070
	Momentum of Inertia of the rotor	[Kgm_2]	6.1

Table 4.3: Generator,SIEMENS 1FW3285-2E

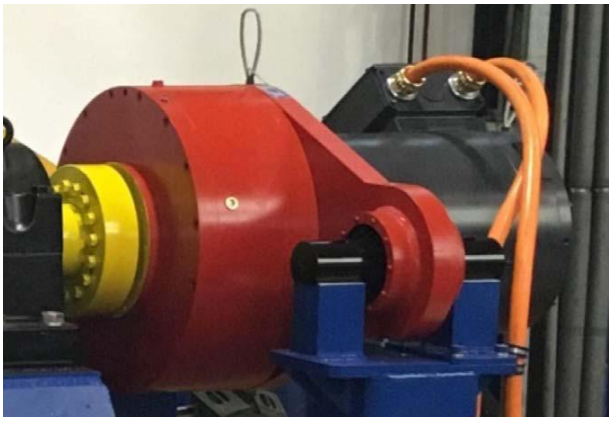

(a) *The PTO: setup of the ISWEC.*

(b) *SIMOTICS T-1FW3 Torque Motor.*

Figure 4.5: PTO Configuration.

4.3.3 The Electric system

The electric system is able to smooth the oscillating power coming from the gyroscope into a more continuous electric power flux to be delivered to the grid. The whole system is supposed to be based on an internal 600V Direct Current(DC) BUS. Some branches

with different aims are linked to this main electric power carrier. The first branch is that of the PTO. This component convert the mechanical power coming from the precession shaft into an oscillating electric power shaft. Its power electronics turns the Alternate Current(AC) electric power coming from the generetor into a DC shape and then throws into the DC BUS. This is the power input for the whole system

The fundamental function of smoothing the cyclical peaks of power absorption is realized by a branch of Ultra Capacitors(UC). For smoothing a variation of 10V with respect the 600V of the BUS line a series of 5 Maxwell UC with nominal working voltage of 125 V and a capacity of 19nF each is used

$$C = \frac{2E_{el}}{(V_0 + \Delta V)^2 - V_0^2} \tag{4.1}$$

where E_{el} is the entrant electric energy and its define as follow:

$$E_{el} = \frac{P_0 T_{nom}}{\pi} \tag{4.2}$$

Where P_0 has been considered equal to the PTO nominal torque previously described, and T_{nom} is the nominal period of the power signal considered equal to 6s.

Then a bidirectional DC/DC converter interfaces the DC BUS with the storage onboard. The installed electrical capacity is made of a group of 10 batteries with 12V rated voltage and 100Ah capacity. They are connected is series in order to reach a Voltage of 120V and a total storage capacity of 12kWh. The model of the battery is 12FLB 250 by FIAMM.

Representing the battery as a parallelepiped its main dimesion are:

dimensions: 272mm x 166mmx 195mm

Here below are then reported the dimension of an equivalent box which represents the space required for the whole storage system.

equivalent box: 544 x 839 x 195

4.3.4 The Floater

Once the functional subsystems have been defined, the cylinder has to be coated in order to make it to float in the sea water and to enhance the wave exitation force. The objective is to coat the cylinder with floaters for having as a final result a buoy floating in the sea. The Resinex catalogue has been taken as a reference for the analysis. They manufacture sea support buoys ranging from 1 meter to 5,8 meters in diameter and can arrive up to over 120tons of net buoyancy thanks to modularity.
They are assembled in polyethene modules filled with polyurethen foam. These floaters are choosen to lay the steel cylinder containing the machinary room. The gyroscopic group is positioned such that the precession axis correspond with the hull vertical axis. In fig 4.6 the final configuration is presented. This configuration have been considered optimal for the advantages introduced in terms of the WEC installation and release time as well as obtaining, at the same time, an increase in safety.
Then the hull is composed by three layers of floaters. In fig.4.7 is shown the final geometry of the hull and are defined the geometric parameter:

- **H**: the overall hull height;
- h_i: the height of the module of i-th layer;
- D_i: the diameter of the i-th layer;

In Tab. 2 is shown the weight distribution of the device: the weight of the pre-defined gyroscopic unit and of the tin cylinder are kept fixed, instead the weight of the hull may vary according to the draft value.

Mass	Unit	Value
Hull	ton	25-48
Tin cylinder	ton	8
Gyroscpe	ton	3

Table 4.4: Floater properties

A comparison between the semi-elliptical profile shape configuration and the new one has been performed in term of productivity. In particular, the plant size has been

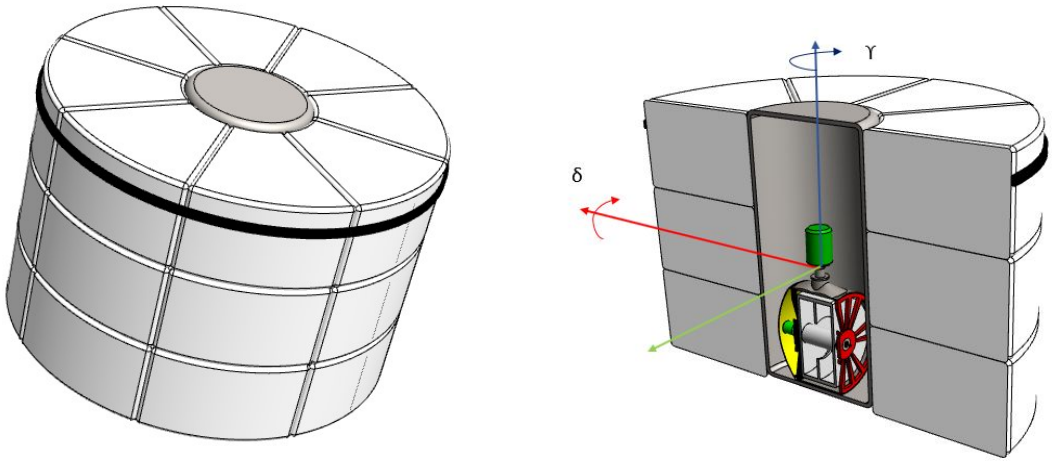

(a) hull **(b)** *complete system*

Figure 4.6: Hull 3-D representation.

compered at different draft values. The mechanical characteristic of the two equivalent floaters are summarized in table 4.5 and 4.6. The dimension of the semi-elliptical hull has been defined considering an overall height almost equal to the cylindrical hull, but at the same time the equivalent radius has been selected greater than $2.5m$ for keeping the general shape of a '*bowl*' that otherwise would have been compromised. The inertia tensor and the coordiantes of the center of gravity of the system compered are considered equal for the comparison. In particular, they have been calculated through Solidworks for the cylinder-shaped floater. The displaced mass has been considered analitically for both the configurations.

Properties group	Quantity	unit	Value
Geometry	Floater equivalent radius(R_{eq})	[m]	3.2
	Draft	[m]	[1.88 2.21 2.54]
	Floater height (H)	[m]	3.2

Table 4.5: Spherical-hull equivalent floater properties for the productivity comparison with the cylindrical cconfiguration.

The hydrodynamic parameters that influence the hydrodynamic behaviour of the floater have been computed throug Nemoh. In the figure 4.8 are shown the 3D mathemathical representation of the floaters, their discretization and the relative mesh for

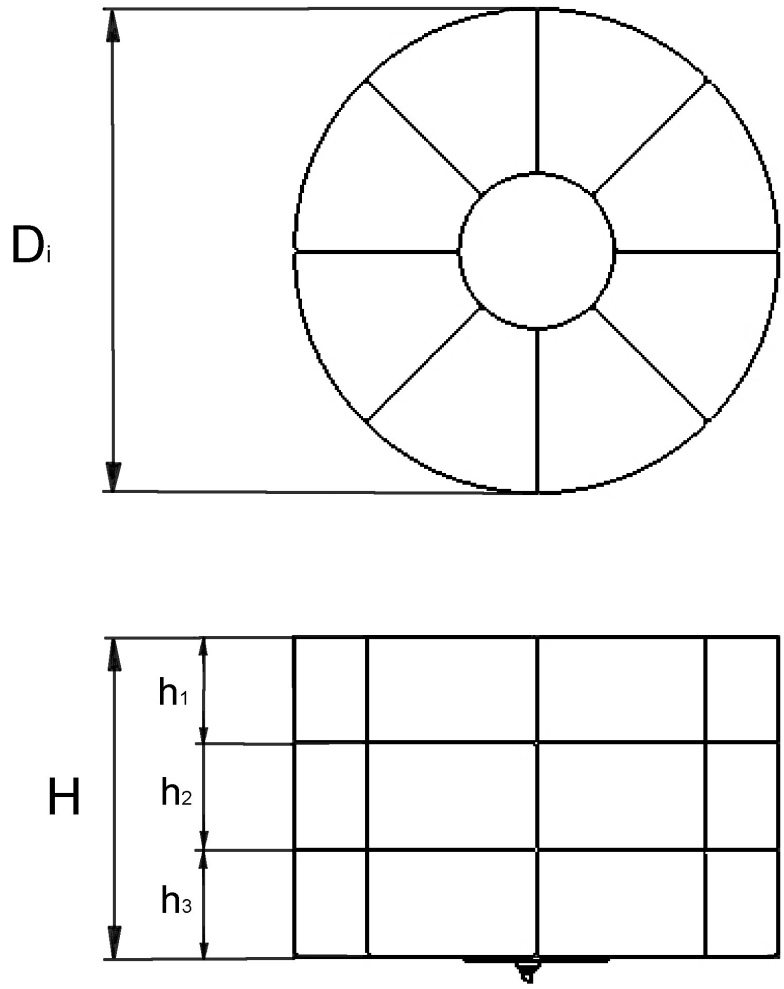

Figure 4.7: Hull parametric definition.

Properties group	Quantity	unit	Value
Geometry	Floater equivalent radius(D)	[m]	2.5
	Draft	[m]	[1.98 2.31 2.64]
	Floater height (H)	[m]	3.3

Table 4.6: Cylindrical Hull geometric parameters definition.

Nemoh.

The results of the productivity for both hull profile are plotted in Figure 4.9, where it is highlighted that the 'bowl' hull is more hydrodynamic than the cylinder. In particular, the productivity for the semi-elliptical hull is about twice the productivity of the new

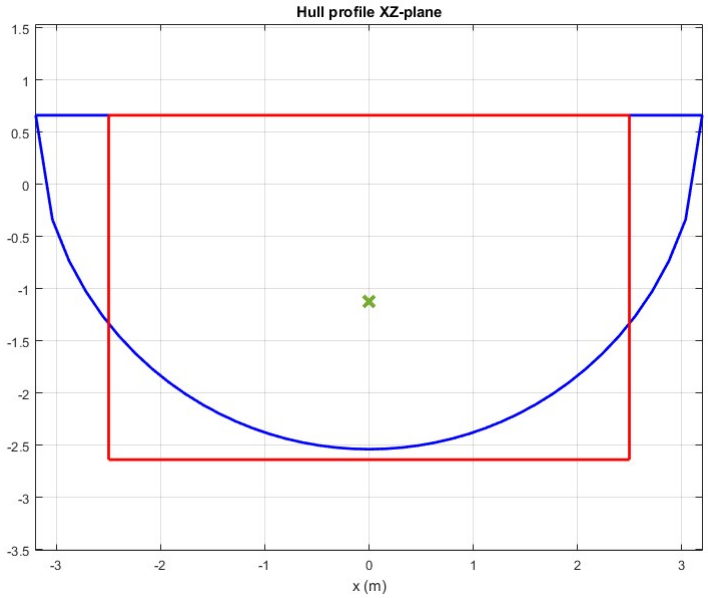

(a) hull

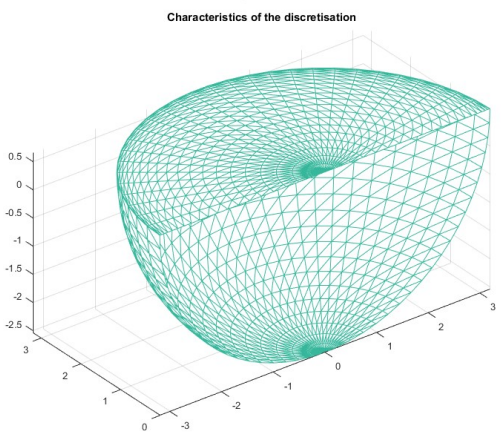

(b) *complete system*

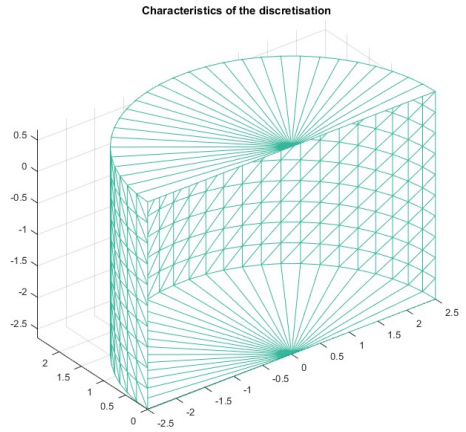

(c) *complete system*

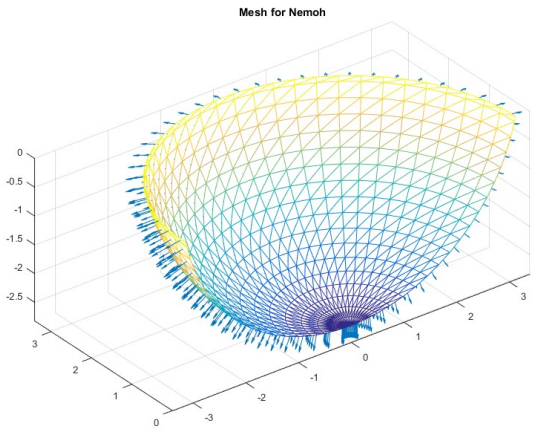

(d) *complete system*

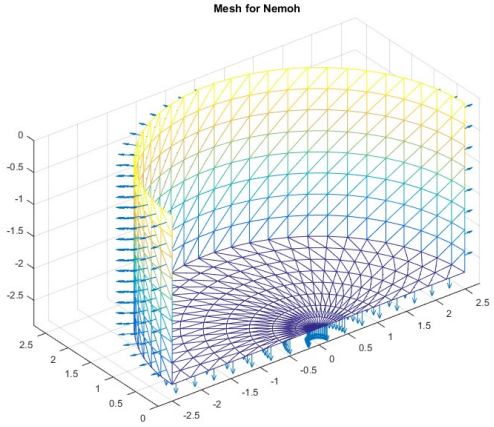

(e) *complete system*

Figure 4.8: Hull set up for Nemoh analysis.

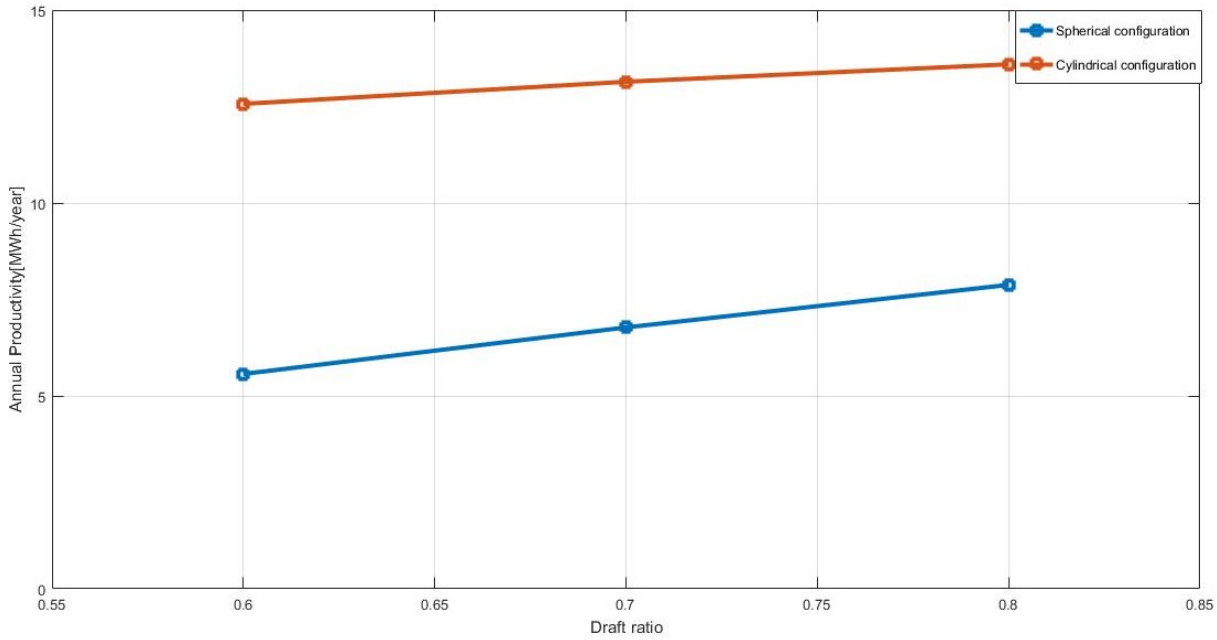

Figure 4.9: Productivity comparison between the 'semi-elliptical' configuration and the 'cylindrical' one.

configuration. For lower draft values such different get more evident. The new configuration considered is a good starting point but the performance requirements in terms of Gross Power produced were not fulfilled. The hull shape, consequently its hydrodynamic wasn't optimal to exploit the incoming wave power. For keeping such a solution still up, in next section is purposed the analysis of several floater modules set up.

4.4 Draft Analysis

The hull draft is one the design parameters of the whole device. The draft is a dimensionless parameters defined as the ratio between height of the submerged part and the total height of the hull. It is hereafter defined:

$$DraftRatio = \frac{H}{draft} \tag{4.3}$$

The draft ratio has a great influence on the dynamic responce of the system. It is an index of the submerged hull volume and then it influences the weight of the device it self which has to counter balance the hydrostatic load applied by the displaced volume. Once the mass changes as a function of the draft ratio, the inertia tensor and the coordinates of the center of mass change as well. The flow diagram below shows the influence of the draft ratio over the parameters which defines the device.

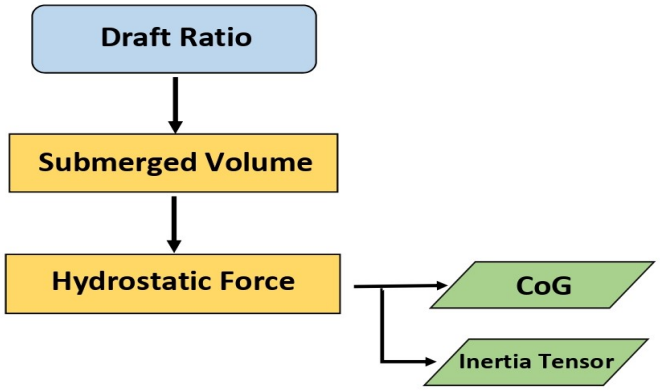

Figure 4.10: Draft ratio analysis.

The draft ratio, knowing the overall height of the floater define the draft of the hull.

$$draft = H \cdot DraftRatio \tag{4.4}$$

The draft of the hull define the submerged volume of the cylinder.

$$Sub.Volume = draft \cdot \pi \frac{D^4}{4} \tag{4.5}$$

Then is possible to evaluated the hydrostatic force acting on the hull counterbalance by

the weight of the hul it-self.

$$HForce = Sub.Volume \cdot d_{sea-water} \cdot g \tag{4.6}$$

where $d_{sea-water}$ is the sea water density equal to $1025 kg/m^3$.
Considering a homogeneous mass distribution of the floater, the CAD program gives the coordinates of the center of mass and the inertia tensor of the hull. The comparison in

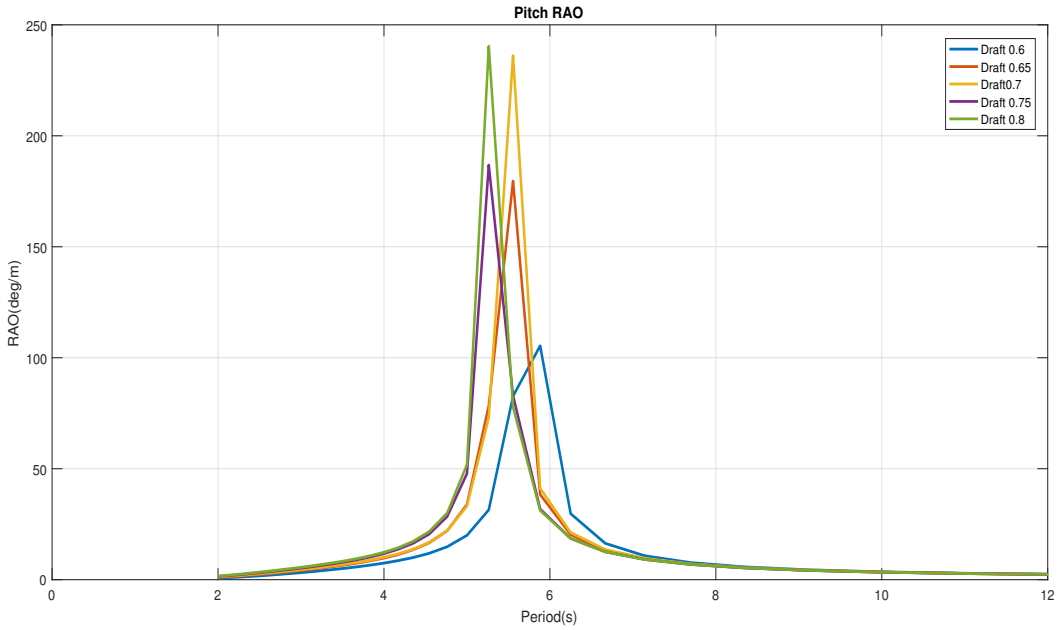

Figure 4.11: RAO analysis for different draft ratio.

term of productivity for different hull configuration is performed. The characteristic of each floater analized are sum up in the Tab. 4.7

Configuration	D_1	D_2	D_3	h_1	h_2	h_3
-	[m]	[m]	[m]	[m]	[m]	[m]
1	5	5	5	1.1	1.1	1.1
2	5	5	4.3	1.1	1.1	1.1
3	5	5	3	1.1	1.1	1

Table 4.7: Floater identification.

As shown in Fig 4.12 the lower output power is expected for the draft ratio equal to 0.6 being its period of resonance close to 6s. It's then highlighted comparing the RAOs

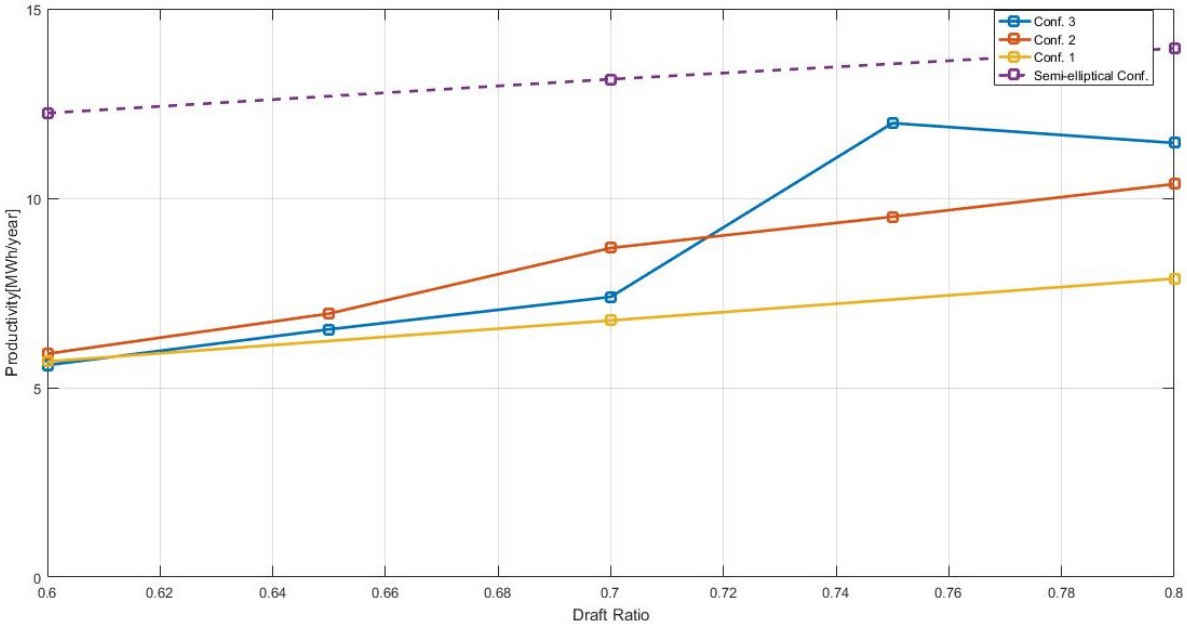

Figure 4.12: Productivity for different floater configuration at diffeent draf ratio.

plot and the annual productivity diagram that the size of the plant increases when the the draf ratio is close to 0.75 or 0.8, when the resonance peack of the linear pitch responce is close to 5s.

4.4.1 Wave analysis

In this paragraph is reported the analysis performed by the ISWEC design tool given one input wave. Once the wave function is defined as Fourier series, the irregular hydrodynamic force is compued and through the state space representation of the system, the pitch responce is defined and consequently the torque and rotation of the precession axis. In particular, once the Froude Krilov coefficient $f(\omega)$ is define dby Nemoh, the irregular hydrodynamic force acting on the system can be calculated in time domain:

$$\tau_w(t) = \sum_{n=1}^{M} F_m cos(\omega_m t + \phi_m + \theta_m) \tag{4.7}$$

Where:

$$F_m = \sqrt{2|f(\omega - m)|^2 S_{\eta\eta}(\omega_m)\Delta\omega} \tag{4.8}$$

$$\theta_m = arg[f(\omega_m)] \tag{4.9}$$

are respectively the magnitude and the phase between the hydrodynamic force and the wave profile relative to the m-th frequency component. $S_{\eta\eta}(\omega)$ is the power density value dependent on the frequency ω. Then in table 4.8 are defined all the input variables and all the system characteristic parameters resulting from the simulation of the device.

Propertie group	Quantity	Unit	Value
Irregular wave	Wave energy period	[s]	5.0522
	Wave significant height	[m]	1.5995
	Wave Power Density	[kW/m]	6.3335
Simulation constraints	δ_{rms}	[deg]	16
	δ_{max}	[deg]	44
	ϵ_{rms}	[deg]	47
	ϵ_{max}	[deg]	127
	$T_{PTO_{rms}}$	[Nm]	832.400
	$T_{PTO_{max}}$	[Nm]	2342.400
Design parameters	c	[Nms/rad]	842
	k	[Nm/rad]	17390
	$\dot{phi}$	[rpm]	196
Simulation output	Device Gross Power produced	[kW]	1.178
	RCW		0.037

Table 4.8: Value of the design parameters.

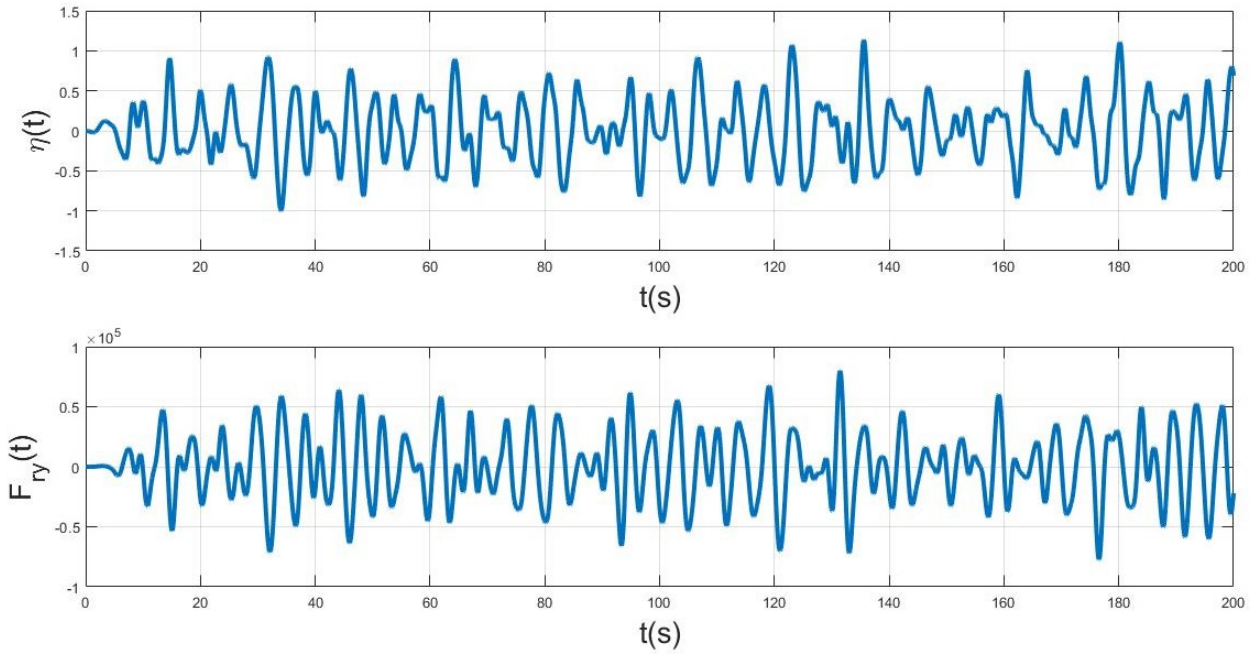

Figure 4.13: Irregular wave elevation and relative hydrodynamic force.

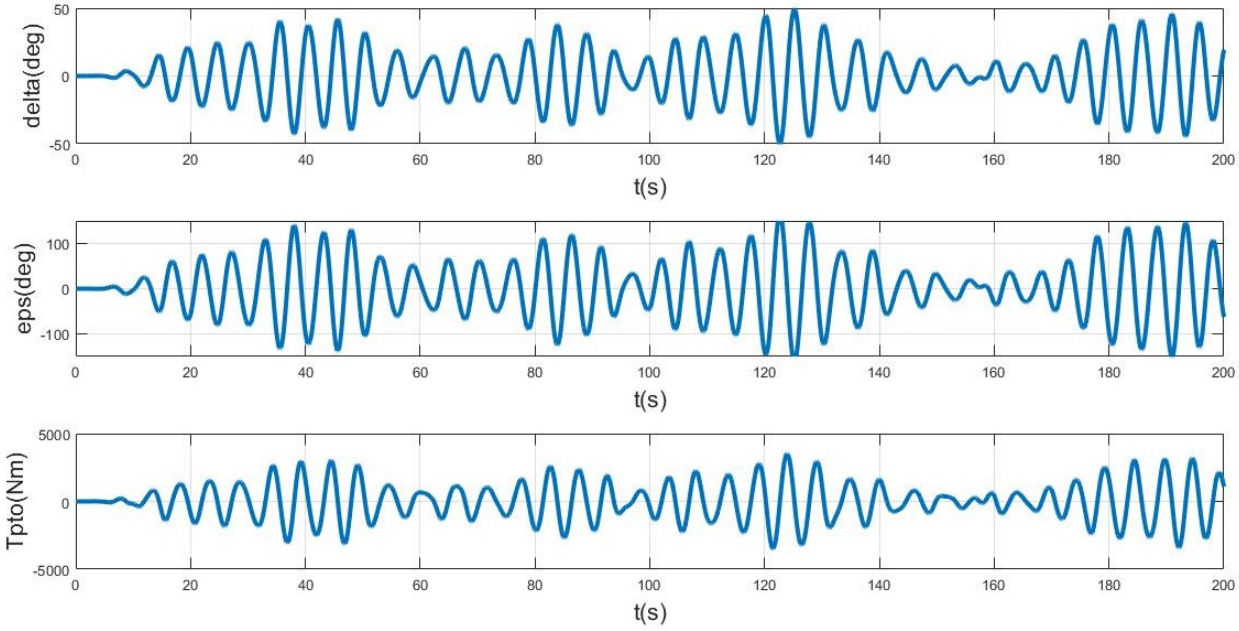

Figure 4.14: Plot of the main system output function.

4.5 Draft Analysis Example

In this section is reported a complete analysis of a floater configuration. Once the draft ratio has been defined, several steps are computed for determining the parameters to set for the productivity computation of the device.

In the diagram of figure 4.15 are sum up all the steps for the evaluation of the char-

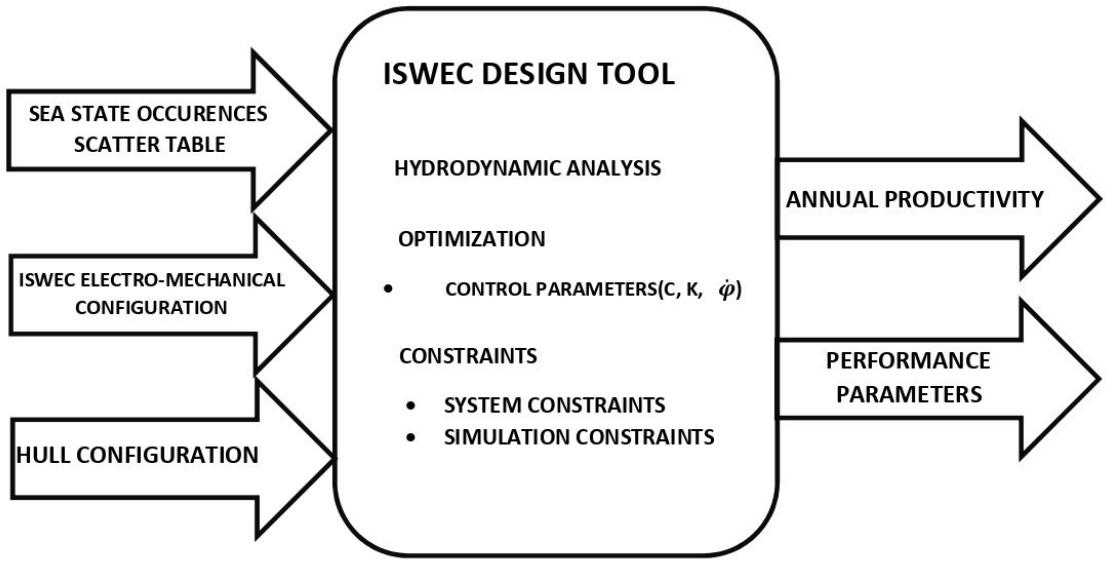

Figure 4.15: IDT flow diagram.

acteristic parameters of the whole plant. Before starting the analysis of the plant it is necessary to define the kind of see it has to be installed. In partcular we are using a reference site the see surface surrounding Pantelleria in the south of Italy. Such a site is well defined by 228 waves that are given as imput to the IDT, but for it is also required to set the 'Occurences Scatter Table' which gives informations about the occurence hours in one year of each characteristic wave. The second step is the definition of the electric system and the gyroscopic units. Finally the hull has to be defined in order to study the conversion of the wave potential energy into mechanical power.

The IDT then performs the hydrodynamic analysis through *Nemoh*, generates the forcing term and through a local optimization algorithm performs for each characteristic wave the value of the control parameters and of the flywheel rotational speed, respecting the

set constaints.

Finally the IDT gives as outputs the matrices of all the design parameters, the performance values of the device and the annual productivity of the device in $MWh/year$. All the parameters for running the simulation of device analized in this section are presented in Table 4.9. It possible to notice taht a new hull configuration has been studied: the main idea was tuo make the hull profile changing along the x and z axis. For this analysis the third layer is composed by a stage of floater having the diameter of 4.3 meters.

Properties group	Quantity	unit	Value
Geometry	Floater Maximum radius(up layers)	[m]	5.00
	Floater Minimum radius(third layer)	[m]	4.30
	Floater height	[m]	3.30
Overall Mass properties	Overall system Mass	[ton]	44.046
	Momentum of Inertia about longitudinal axis x	[kg m^2]	99243
	Momentum of Inertia about transversal axis y	[kg m^2]	98986
	Momentum of Inertia about vertical axis z	[kg m^2]	113422
Hydrostatic properties	Draft ratio		0.75
	Period of Resonance	[s]	5.126
	Submerged Volume	[m^3]	42.971
	z-coordinate of the center of mass	[m]	-0.824

Table 4.9: Floater properties

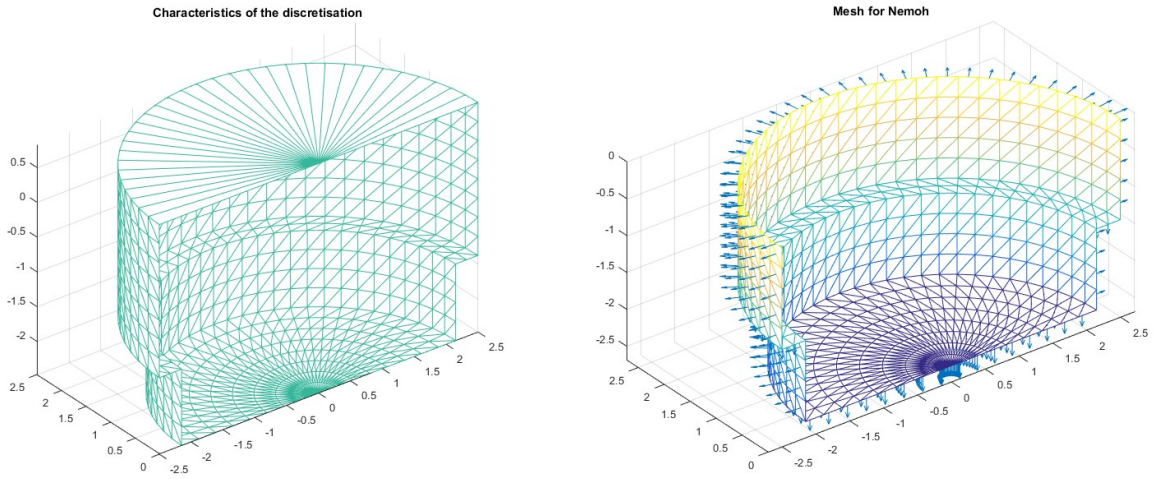

(a) hull **(b)** *complete system*

Figure 4.16: Device rapresentation $\mathcal{B}$.

In particular, the hydrodynamic properties of the floater computed by Nemoh are:
-Added Mass tensor A(frequency dependent)
-Damping coefficient tensor B (frequency dependent)
-Stiffness tensor K
The stiffness matrix is:

$$K = \begin{bmatrix} 0 & 0 & 0 & 0 & 0 & 0 \\ 0 & 0 & 0 & 0 & 0 & 0 \\ 0 & 0 & 197120 & 0 & 0 & 0 \\ 0 & 0 & 0 & 166630 & 0 & 0 \\ 0 & 0 & 0 & 0 & 166630 & 0 \\ 0 & 0 & 0 & 0 & 0 & 0 \end{bmatrix}$$

The hydrodynamic properties of the floater can be presented using the linear model hypothesis already presented in chapter 2 and whose synthetic result is the response amplitude operator, the RAO.This is a common instrument for the analysis of stability in ship industy and for designing floater in wave energy field. The pitch responce is required to be as close as possible to the main wave period of the sea where the device is going to be installed. Thus, the wave period in which the floater is designed to maximize the oscillation is T=5s. The mass, geometric and hydrostatic properties are summarised in table 3.1.

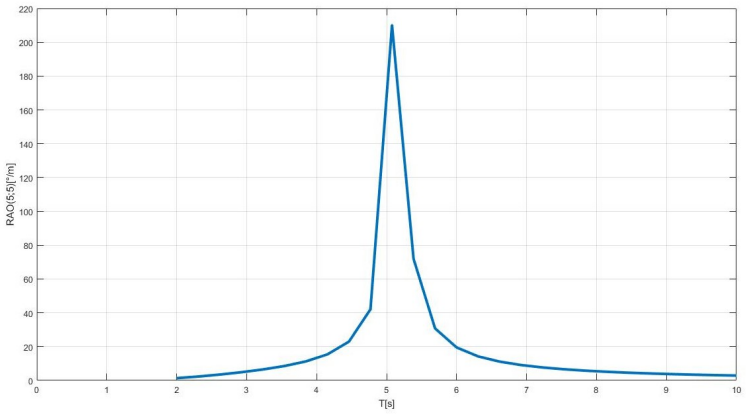

Figure 4.17: Floater dynamic responce. The pitch RAO with fully linear BEM modelling approach.

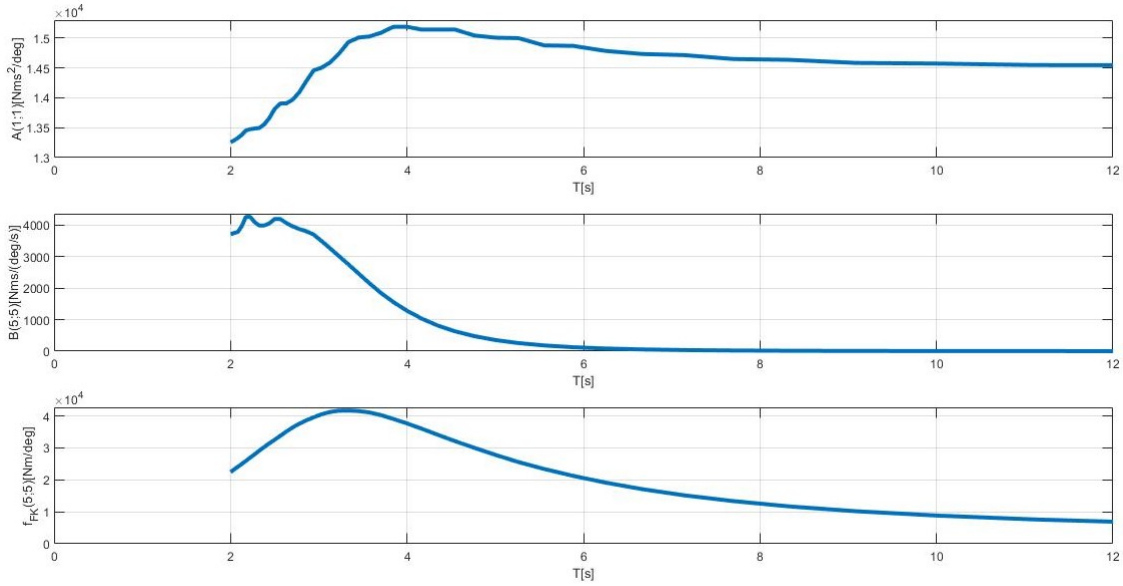

Figure 4.18: Device annual productivity.

The simulated system resuts to be a 2.5kW plant, and the resulting annual productivity is of 11.325MWh/year. In the table below are shown the maximum value of the matrices resulting from the optimization. The hydrodynamic result of this hull configuration are reported below.

Properties group	Quantity	Unit	Upper bound	Max. Value
Design Parameters	c	[Nms/rad]	10^5	71910
	k	[Nm/rad]	10^5	95600
	$\dot{\phi}$	[rpm]	1500	1500
Simulation constraints	ϵ_{rms}	deg	70	63.43
	δ_{rms}	deg	20	18.97
	$T_{PTO_{rms}}$	[Nm]	3500	2495

Table 4.10: Maximum values of the design parameters.

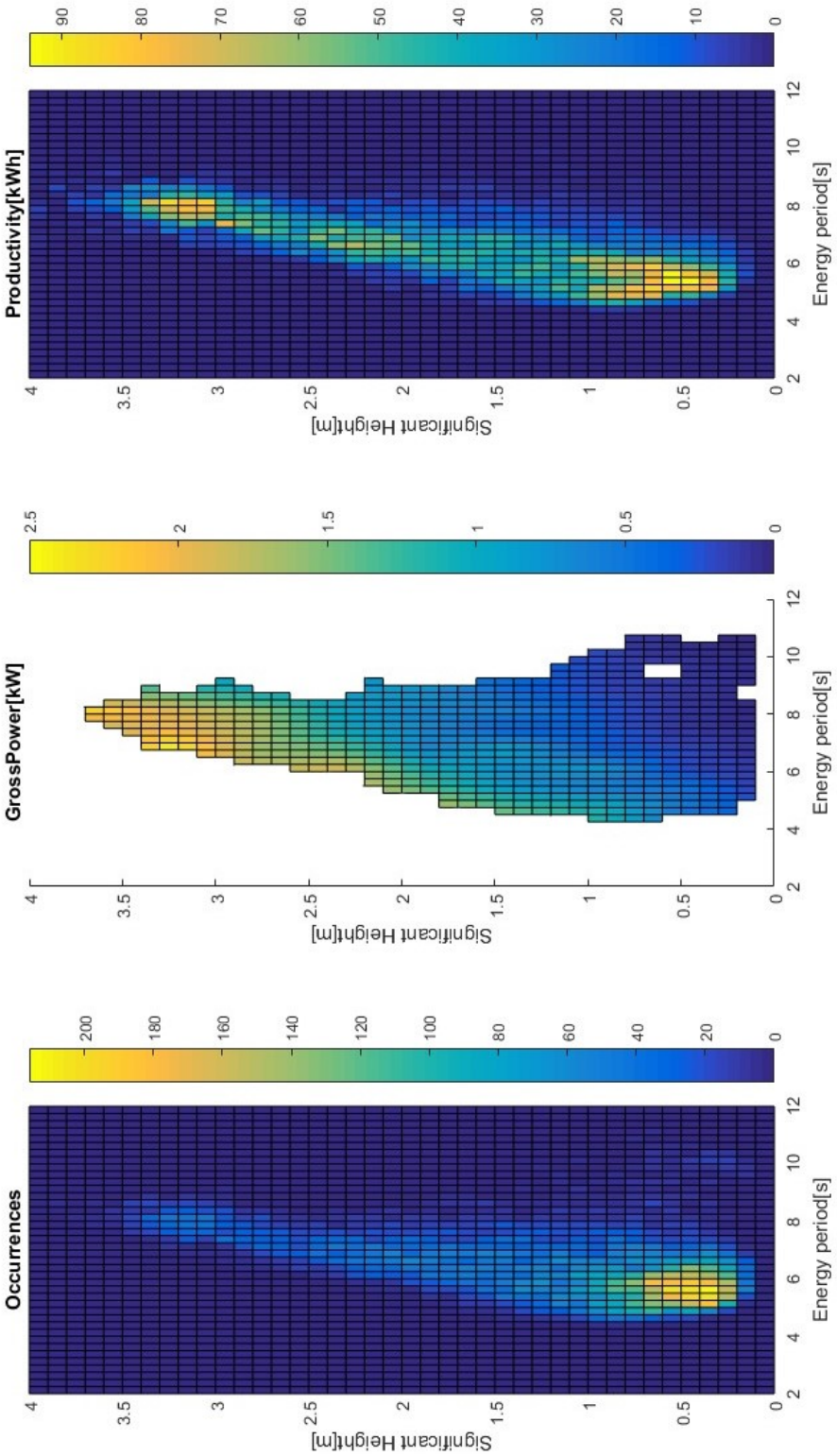

Figure 4.19: Device annual productivity.

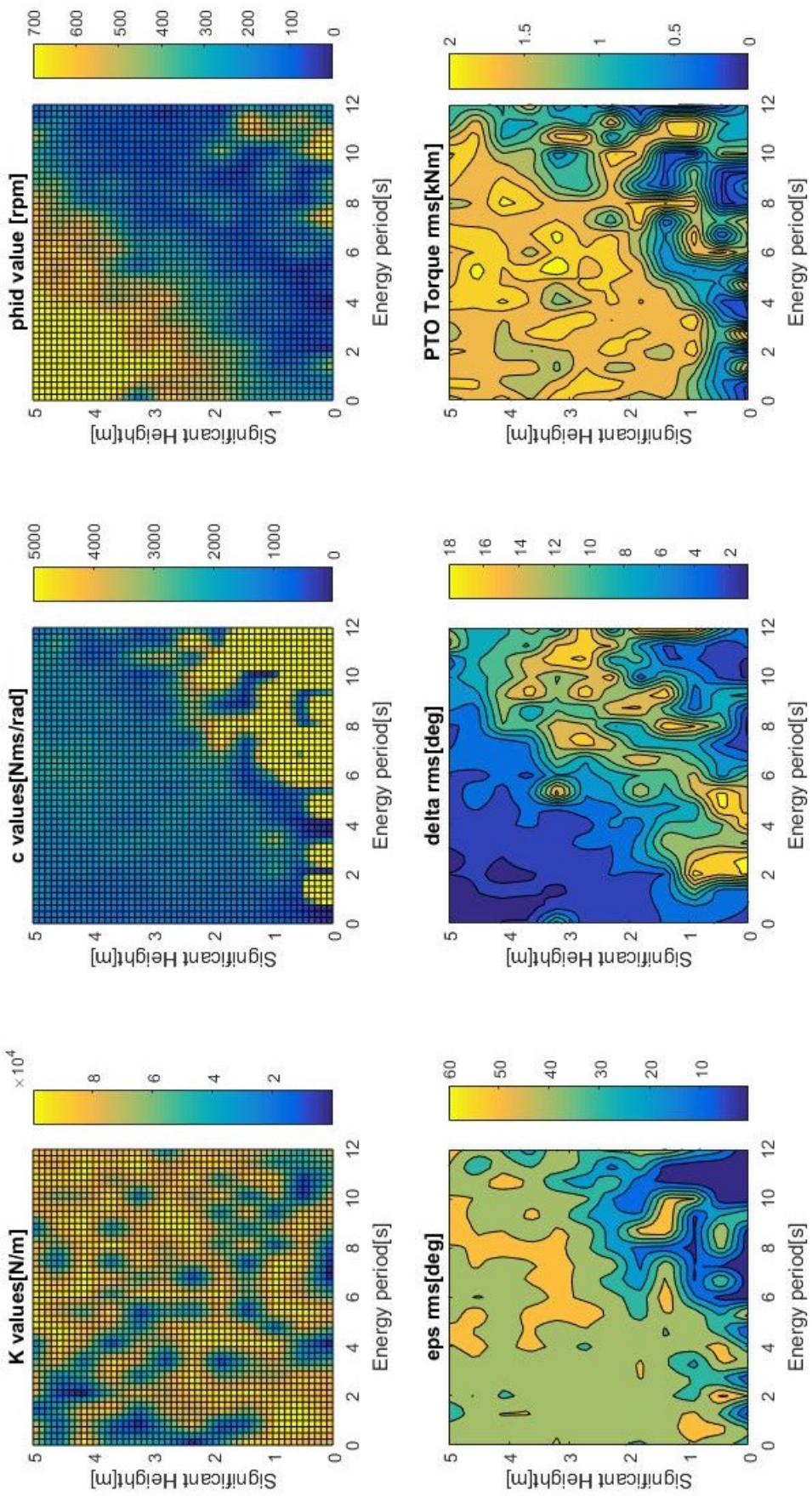

Figure 4.20: Design parameters and performance results.

Chapter 5

Hydrodynamic validation

The study of the body dynamic in a fluid is the most important part to be described in this kind of application, beacause of the nature of the system input. In the ISWEC design presented in previous chapter Nemoh tool has been used to extrapolate the dynamic properties of the floating body in the sea water. This kind of approach as been choosen because of its feasability in Matlab environment: characteristics which make possible to the designer to study different device configurations in an automatic way.
In this chapter, a comparison is made between the key device parameters of a precise hull configuration, using the well-established, commercial BEM solver ANSYS AQWA and the open-source BEM solver, NEMOH. Both approach are limited by the linear nature of the potential flow theory, but the speed with which numerical simulation may be performed compared to other simulation method, such as computational fluid dynamics(CFD), makes BEM a common choise for early stage device development. After checking that NEMOH shows good overall agreement with WAMIT[5](the most used commercial BEM), it can be explored its accordance with AQWA. Ansys Aqwa software is an engineering analysis suite of tools for the investigation of the effects of wave, wind and current on floating and fixed offshore and marine structure. As shown in fig. 5.1, the analysys, comparison and validation of the IDT(Iswec Design Tool) will be performed over two stages:

- Hydrodynamic parameter computation for Nemoh validation. Ansys Aqwa Difraction analysis wil be computed for developing the primary hydrodynamic parameters required for undertaking complex motion and responce analysis.

- Time responce analysis of the hull under an irregular wave excitation for the validation of the IDT state space representation.

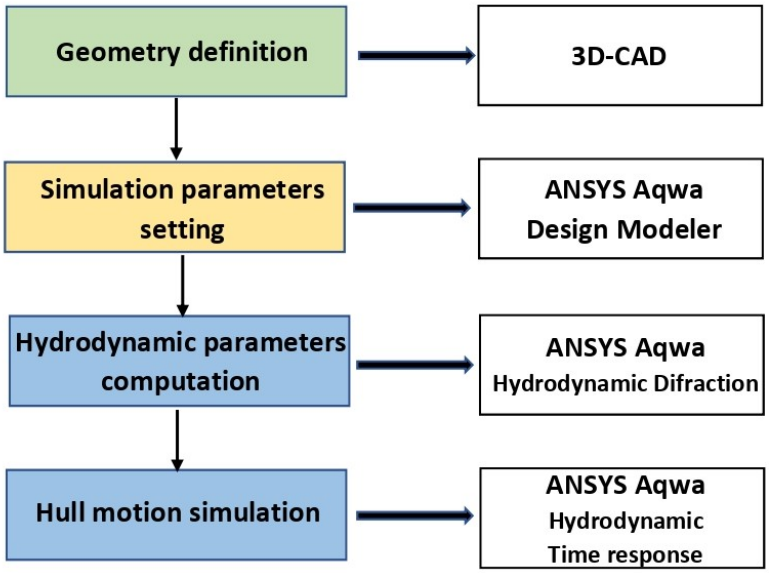

Figure 5.1: Ansys validation steps.

5.0.1 Difraction Analysis

In order to start the simulation in Ansys Aqwa environment it is required to define the geometry, then the hull shell has been modelled on Solidworks and exported. Once the geometry is defined it is required to separate the body surface into two layers according to the water level and to define the Inertial property of the floater. For the comparison has been taken as a reference the hull described in the previous chapter in the $DraftAnalysisExample$ section. In table 5.1 are specified the mesh set up of the two methods, taking into account that NEMOH includes a limitation for the number of panels(2000 panels) and AQWA guarantees a robust solution for a number of panels grater than 3000. The NEMOH-Mesh is composed of flat quadrangular panels and then only the submerged part of the body is described. One way for generating mesh on Nemoh is to use axiMesh.m to generates an axisymmetric mesh with Matlab. Instead, in Aqwa is not possible to employ the symmetry, hence the full model must be meshed. The frequency

Property	Nemoh	Aqwa
Difracting nodes	1410	3368
Difracting elements	1334	3313
Computation time	343s	805s

Table 5.1: Nemoh and Aqwa mesh generation comparison and running time.

range of the analysis for Nemoh and Aqwa has been performed considering a frequency vector of 47 element with $2s$ and $25s$ as lower and upper bound respectively.

As it can see, the NEMOH and ANSYS AQWA analysis is comparable and the results achieved remain consistent. The hydrostatic stifness matrix is slightly inferior with NEMOH calculation, but they are still close each other. Generally the behaviour of the hydrodynamic parameters computed by the two method is pretty similar for the three degree of freedom considered. By the way some error between NEMOH and AQWA has to be highlighted especially for the Froude-Krilov coefficient for the low value of the period T.

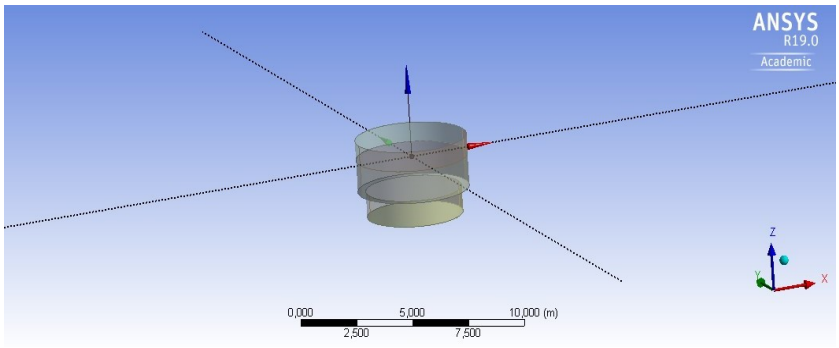

(a) *Ansys: geometry definition*

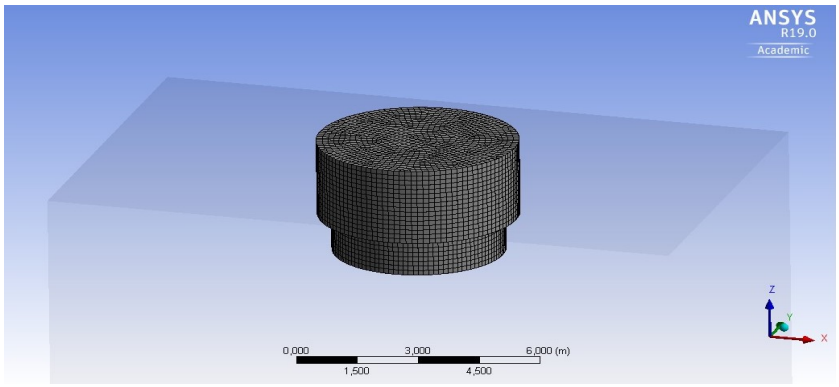

(b) *Ansys: mesh generation*

Figure 5.2: Device rapresentation $\mathcal{B}$.

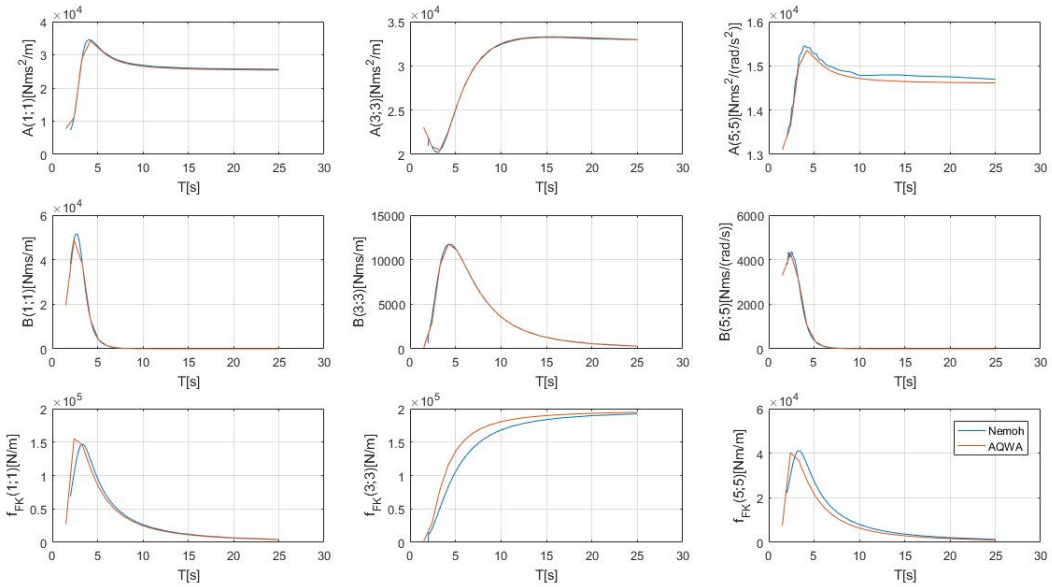

Figure 5.3: Gross Power as a function of Wave Power density.

$$K_{ansys} = \begin{bmatrix} 0 & 0 & 0 & 0 & 0 & 0 \\ 0 & 0 & 0 & 0 & 0 & 0 \\ 0 & 0 & 197255.28 & 0 & 0 & 0 \\ 0 & 0 & 0 & 2946.1902 & 0 & 0 \\ 0 & 0 & 0 & 0 & 2946.1934 & 0 \\ 0 & 0 & 0 & 0 & 0 & 0 \end{bmatrix}$$

Instead, the RAOs plot do basically overlap each other and therefore it is reasonable to

Element	Unit	Aqwa	Nemoh	K_{aqwa}/K_{nemoh}
K(3,3)	N/m	197255	197120	1.0007
K(4,4)	N/rad	168878	166630	1.0134
K(5,5)	N/rad	168878	166630	1.0134

Table 5.2: Nemoh and Aqwa stiffness matrix comparison

apply Nemoh method for this kind of analysis.

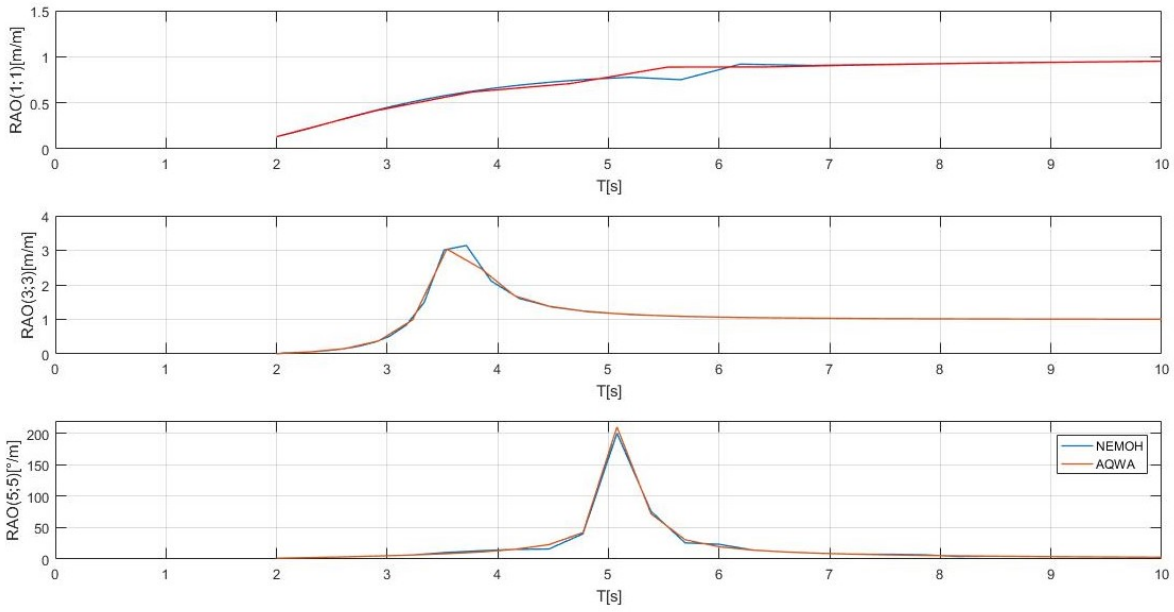

Figure 5.4: Device annual productivity.

5.1 Hydrodynamic Time-responce Analysis

Once the hydrodynamic parameters has been computed as a function of the period, is then possible to evaluate theresponse of the hull under the wave excitation. The response we are going to analize is in time domain, in particular the simulation cover a time interval of 1200 seconds. The time domain analysys is performed in Ansys thanks to the $HydrdynamicTime - Response$ suite. This study has the aim to validate the 3D State Space representation set in the IDT on Matlab. Several hyphotesis have been done:

- The viscous damping force is null;
- The force due to the mooring action has is neglected;
- The drift force is null;

Then the force considered on the system are:

- The hull inertial force;
- The restoring force;
- The radiation force;
- The difraction force;

For the validation of the State Space representation the pitch and heave motion of the hull are the subject of the analysis. The comparison is computed on the basis of sixteen differen irregular waves. They can be added to the Hydrodynamic Time Response system[8]. For reproducing all the wave selected fo the simulation has been required to define the Joswap spectrum in terms of the parameters of **Significant Wave Height**(H_s), **Peak frequency**(ω_p)(the frequency at which the spectral energy is a maximum), and the peak enhancement factor whis has been set to one for all the wave. In figure 5.5 an example of the generated wave on Aqwa is shown.

For both the heave motion the error of the mean square values of the resulting function on AQWA and the IDT is defined as follow:

$$RE_\delta = \left| \frac{\delta_{rms_{ANSYS}} - \delta_{rms_{IDT}}}{\delta_{rms_{ANSYS}}} \right| \tag{5.1}$$

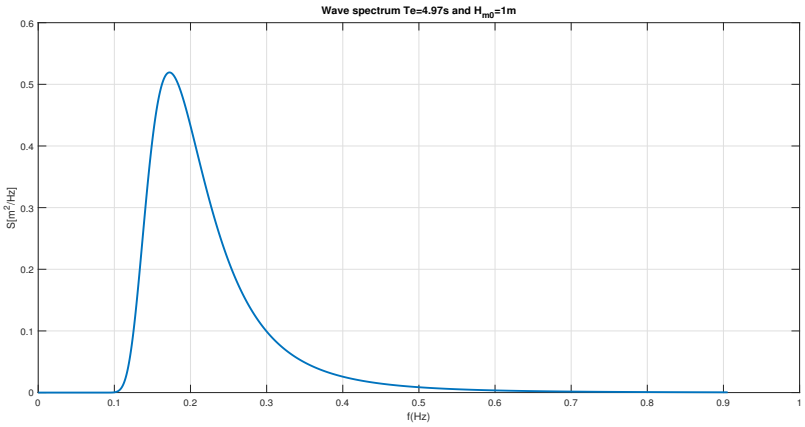

(a) *AQWA wave spectrum representation.*

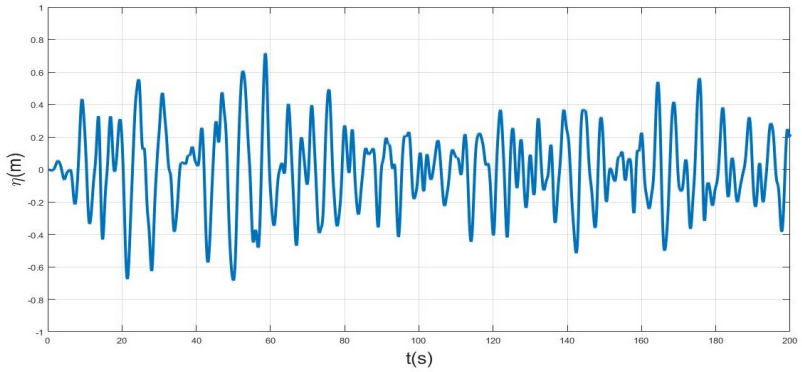

(b) *AQWA wave time series representation*

Figure 5.5: Irregular wave model on AQWA-$T_p = 5s$, $H_m = 1m$.

About the pitch motion the error of the two mean square values of the resulting function on AQWA and the IDT is defined as follow:

$$RE_\delta = \left| \frac{z_{rms_{ANSYS}} - z_{rms_{IDT}}}{z_{rms_{ANSYS}}} \right| \tag{5.2}$$

From the plotted results is possible to notice that the relative error may vary from about 1% to about 15% for the pitch DoF or up to the 20% for the motion along the $z - axis$. Considering that all the considered force are those due to the hydrodynamic of the device, can be state that the error is determined by the difference reported between NEMOH and AQWA when computing the Froude-Krilov coefficient.

T_e[s]	H_{m0}[m]	$\delta_{rms_{IDT}}$[deg]	$\delta_{rms_{ANSYS}}$ [deg]	RE_δ
4.9786	0.5995	18.4216	15.5678	0.1549
5.4936	0.5995	14.0278	15.0821	0.0699
6.0087	0.3997	11.4591	11.7876	0.02787
6.5237	0.5995	12.7231	14.9560	0.1493
4.9786	0.9992	29.0252	24.2313	0.1651
5.4936	0.9992	30.2110	31.0580	0.02727
6.0087	0.9992	25.5351	28.1078	0.09153
6.5237	0.9992	19.0756	21.2178	0.1009
5.0522	1.5995	22.2269	20.6189	0.07798
5.4988	1.5995	24.2269	23.3615	0.0370
6.0087	1.5987	26.0774	24.4403	0.0669
6.5237	1.5987	18.8378	19.6594	0.04179
5.0524	1.9995	32.5307	29.8132	0.0911
5.4551	1.9995	18.5307	19.6594	0.0574
6.0247	1.9995	36.5307	37.0554	0.0141
6.5237	1.9995	34.2806	30.3795	0.1267

Table 5.3: IDT ans AQWA pitch rms values.

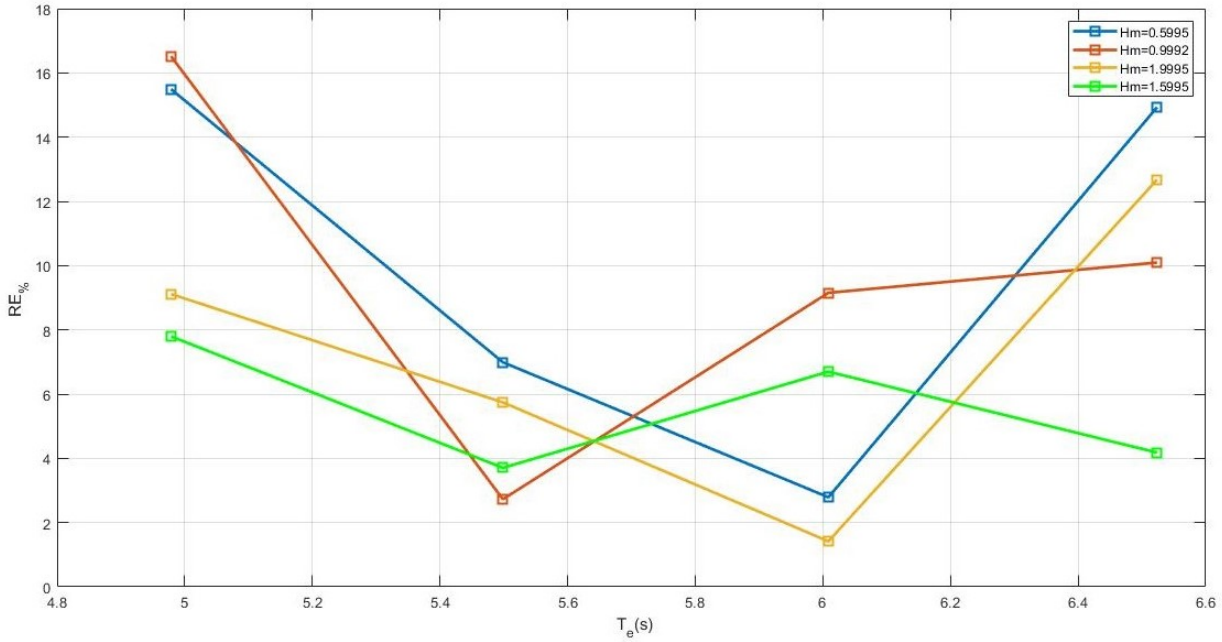

Figure 5.6: IDT and AQWA pitch time respose comparison.

T_e[s]	H_{m0}[m]	$\delta_{rms_{IDT}}$[deg]	$\delta_{rms_{ANSYS}}$ [deg]	RE_δ
4.9786	0.5995	0.1792	0.2052	0.1424
5.4936	0.5995	0.1572	0.1655	0.0526
6.0087	0.3997	0.1182	0.1370	0.1592
6.5237	0.5995	0.1697	0.1904	0.1218
4.9786	0.9992	0.2994	0.3038	0.0146
5.4936	0.9992	0.3303	0.3104	0.0640
6.0087	0.9992	0.3100	0.3526	0.1374
6.5237	0.9992	0.2898	0.3118	0.0757
5.0522	1.5995	0.3158	0.3243	0.0271
5.4988	1.5995	0.3793	0.4079	0.0756
6.0087	1.5987	0.4313	0.5196	0.2048
6.5237	1.5987	0.4463	0.4291	0.0401
5.0524	1.9995	0.3621	0.3807	0.0513
5.4551	1.9995	0.4603	0.48147	0.0458
6.0247	1.9995	0.7527	0.71244	0.0566
6.5237	1.9995	0.5457	0.6043	0.1072

Table 5.4: IDT and AQWA heave rms values.

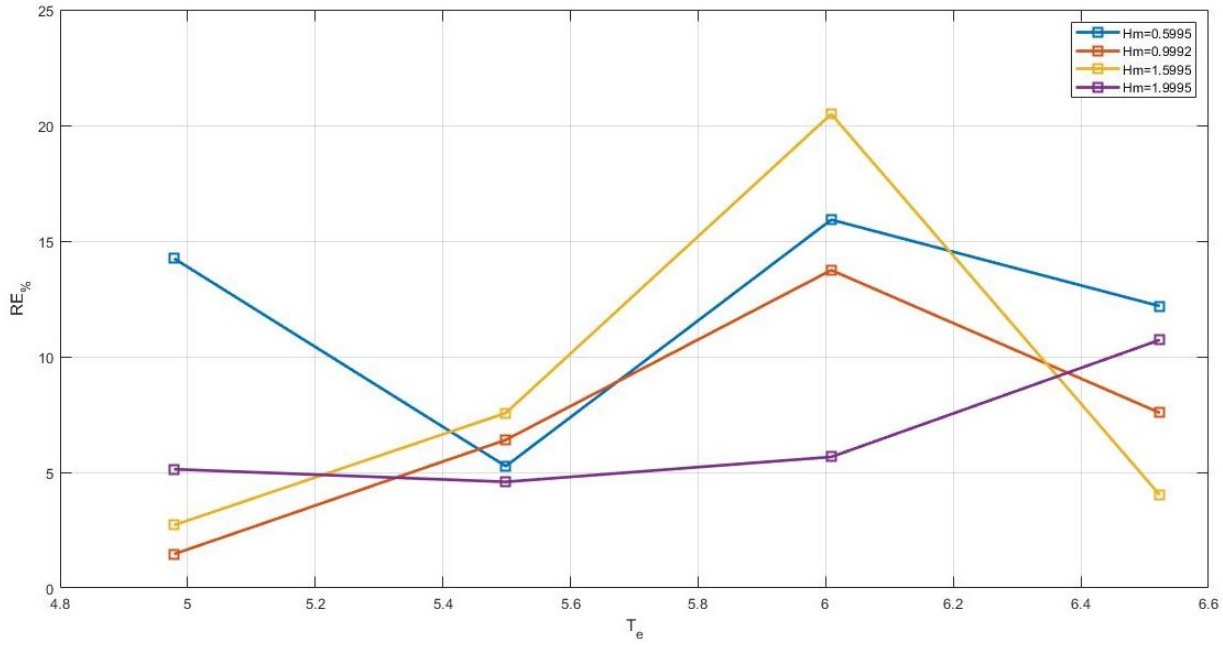

Figure 5.7: IDT and AQWA heave time respose comparison.

5.2 Yaw Moment Analysis

In this section a frequency analysis of the system will be carried out. From the state space representation of the system all the transfer function releted to the yaw rotation of the hull will be obtained and Bode diagrams of such tranfer function are plotted. The aim of this section is to analize the yaw rotation of the hull induced by the wave force and by the inertial totation determined by the PTO system which may induce an indesirable rotation with respect the z axis of the whole device.

5.2.1 Yaw Moment Analysis

The device under the action of the wave exiting force which direction is parallel to the x results in one rotation motion of the hull with respect the y axis(pitch motion) and two displacement motion(surge and heave).These enounced are then the state variables introduced in the 3-DOF model OF the ISWEC-Omnirectional tool presented in Chapter 2.

A special focul is required by the yaw rotation of the hull.It is negligible considering the hull and exitation force acting on the x direction.

The system get different during the work condition and when the inertial rotation of the gyroscope with respect the procession axis get considerable and may cause a rotation of the whole hull body.As discussed in the previous Chapter the equation of a rigid floating marine structure with zero forward speed can be written, in LSA is:

$$(I_h + A_\infty)\ddot{X} + \int_a^b h_r(t-t')\dot{X}dt' + B_{visc}\dot{X} + KX = F_w + F_m + F_c \tag{5.3}$$

then this equation written with respect the yaw rotation,which is the sixth element of the state variables vector X is:

$$(I_h + A_\infty)\ddot{\psi} + \int_a^b h_r(t-t')\dot{\psi}dt' + B_{visc}\dot{\psi} = T_\epsilon \tag{5.4}$$

The stiffness effect linked to the yaw rotation oh the hull is null, any wave acts to rotate the hull and the mooring effect is not consider as a first analysis. Is the torque acting on the precession axis which may cause a rotation of the hull.

Applying the Laplace transfor to the equation 5.8:

$$(I_h + A_\infty)\bar{\psi}s^2 + B_{hydro}s\bar{\psi} = \bar{T}_\epsilon \tag{5.5}$$

Then considering an open loop system where the torque on the precession axis is controlled by a PD controller the equation in frequency domain are:

$$\begin{cases} K\bar{\epsilon} + Cs\bar{\epsilon} = I_g s^2\bar{\epsilon} + J_g\dot{\phi}s\bar{\epsilon} \\ (I_h + A_\infty)\bar{\psi}s^2 + B_{hydro}s\bar{\psi} = J_g\dot{\phi}s\bar{\epsilon} \end{cases} \tag{5.6}$$

The aim of this analysis is the design of a damping parameter C that acting on the dynamic of the system has to reduce the oscillating motion of the hull with respect the z axis. Then:

$$(I_h + A_\infty)\bar{\psi}s^2 + (B_{hydro} + C_{yaw})s\bar{\psi} = I_g s^2\bar{\epsilon} + Cs\bar{\epsilon} + K\bar{\epsilon} \tag{5.7}$$

where B_{hydro} is the equivalent damping coefficent which takes in account the hydrodynamic radiation damping and the damping due to the viscous effects.
Hereafter is reported the transfer function between the yaw rotation $\bar{\psi}$ and the torque T_ϵ:

$$\frac{\bar{\psi}}{\bar{\epsilon}} = \frac{I_g s^2 + cs + k}{(I_h + A_\infty)s^2 + (B_{hydro} + C_{yaw})s} \tag{5.8}$$

The CFD analysis on AQWA have been permormed for estimating the value of the added mass and radiation damping coefficent with respect the yaw motion. It is possible to notice that such hydrodynamic effect is negligible. Hereafter are plotted the results.

The viscous term of the damping can be determined empirically only, then it is not considered as a first analysis, then the resulting transfer function is:

$$\frac{\bar{\psi}}{\bar{\epsilon}} = \frac{1}{C_{yaw}} \frac{I_g s^2 + cs + k}{s(1 + \frac{I_h}{C_{yaw}}s)} \tag{5.9}$$

Then due the function representing the prrcession axis rotation with respect the vertical axis, it is possible to determine the resulting rotation of the hull. C_{yaw} is a damping term that has to act on the system for attenuating the effect caused by the inertial rotation of the PTO axis. C_{yaw} might be the viscous friction coefficent or any other external solution for limitate such a disturbance input on the system. For the analisis purposed here the aim is to understand the beahaviour of the hull considerang a generic damping action.
The transfer function of Eq. 5.9 highlited the pole in zero, which will cause a delay on the responce of the system, and the time constant defined as the ratio between I_h and C_{yaw}.

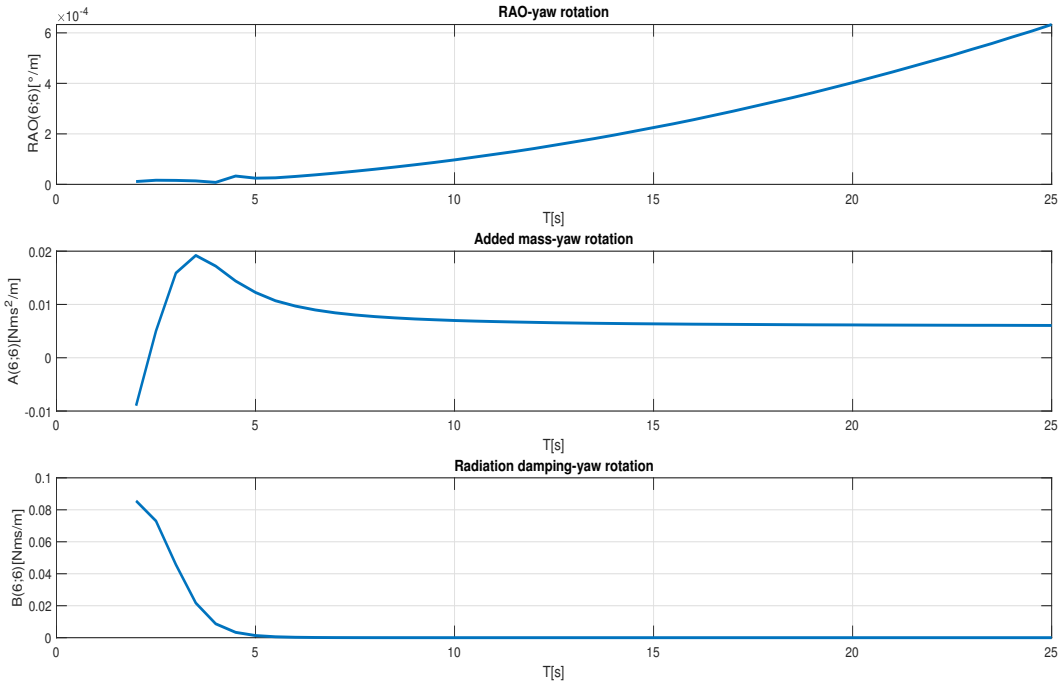

Figure 5.8: Wave spectrum

The highest is C_{yaw}, the shortest is the transient of the system and the most attenuate are the oscillations. All of this aspect are better presented here below.
Let's first define the behaviuor of the system considering the regular wave input. It is define as a sine wave function characterized by the amplitude parameter $(H/2)$ and the the frequency of oscillation (ω_n). Here below the regular wave function is defined.

$$\eta(t) = \frac{H}{2} sin(\omega t) \tag{5.10}$$

Let's in detail see the effect of the input wave on the system. In particular, the wave motion cause a pitch motion of the hull which cause a Torque and then a rotation about the precession axis. All the function are rappresented in Figure 5.10. the parameters fixed for the simulation are the following:

- c= 5'000 Nms/rad
- k= 70'000 Nm/rad
- $\dot{\phi}$= 30 rad/s

- H= 1m
- T= 5,5s

The period of all the resulting function of the system is the the one defined by the wave, but the system behave as an amplified considering the difference in amplitude between the hull oscillation and the ϵ amplitude.
once the linear behaviour of the system has been briefly define, we can compute an analysis in the frequency domain the sixth degree of fredoom of the syste. The bode diagram of the closed-loop transfer function is plotted in the next figure. It is studied the frequency responce of the system varying the C_{yaw} parameter.

The dashed line represents the Bode diagram of the system which C_{yaw} is null. Such system is instable and would diverge to an infinte value of the amplitude. From the diagram is possible to notice that the higher is the damping coefficent the higher is the cut of frequency. Considering that all the oscillation will be in the range between 5s to 10s, we are intesred in filtering the frequency higher to 0.1Hz. Instead, considering the phase Bode diagram the yaw oscillation of the system is out of phase with respect the input signal and in particular it increases when C_{yaw} gets bigger as well.
Then the pole in 0 cause a delay in the responce of the system and C_yaw has effect on the attenuation of the input signal and on trasient time of the syste. This is shown in Fig. 5.12.

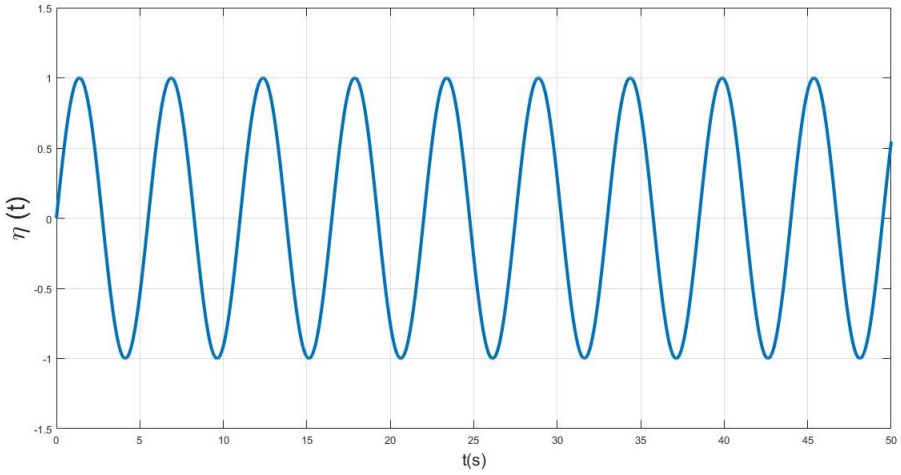

(a) Regular wave function.

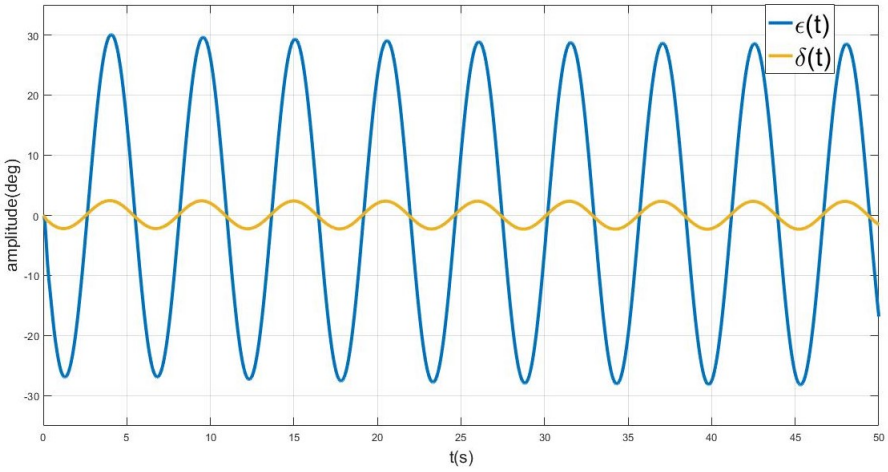

(b) *wave-hull-gyro interaction.*

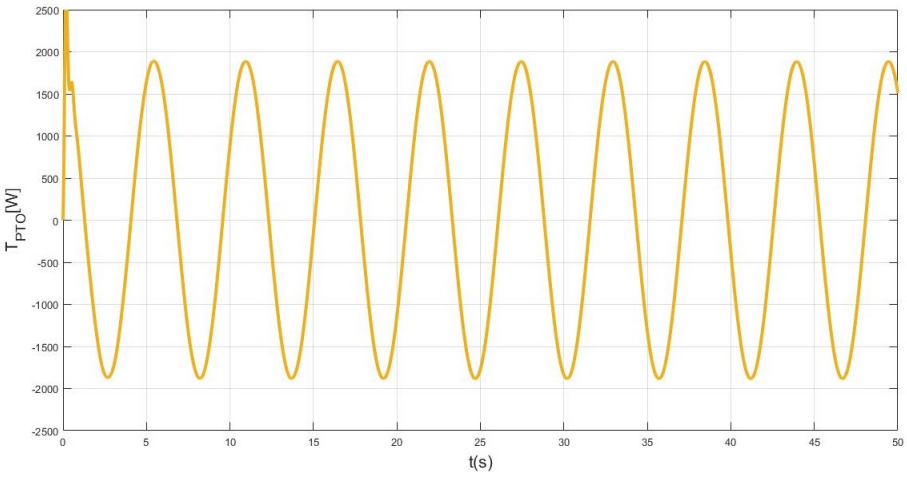

(c) *PTO output Torque function.*

Figure 5.9: Regular wave analysis.

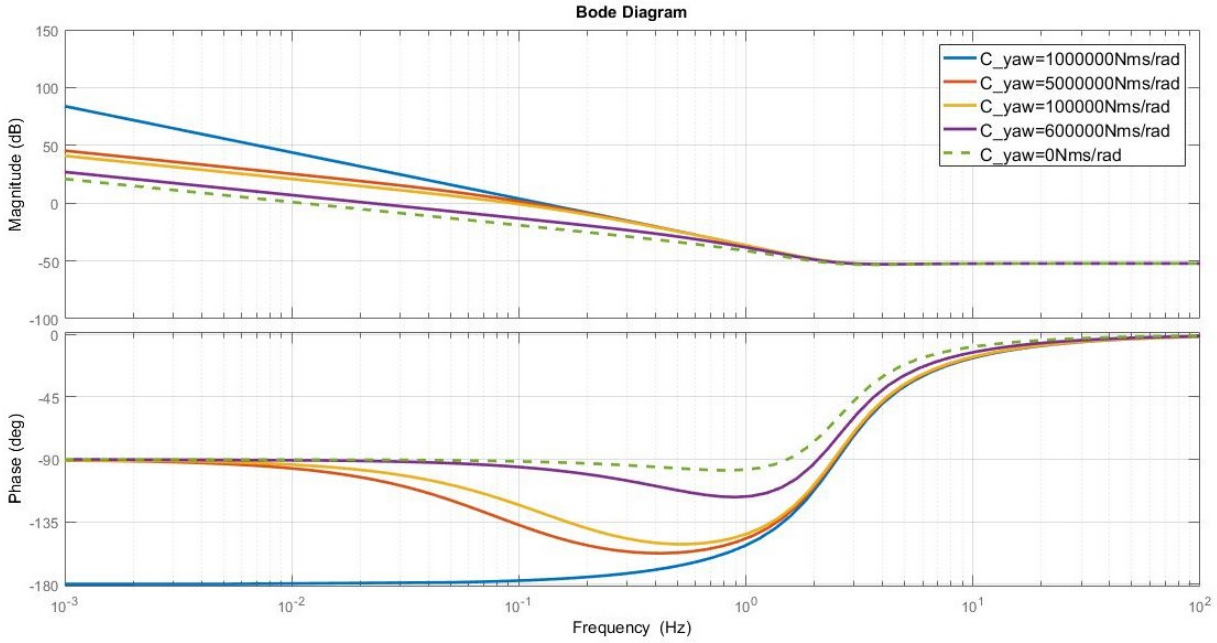

Figure 5.10: Closed loop Bode diagram of the hull yaw motion-Damped response.

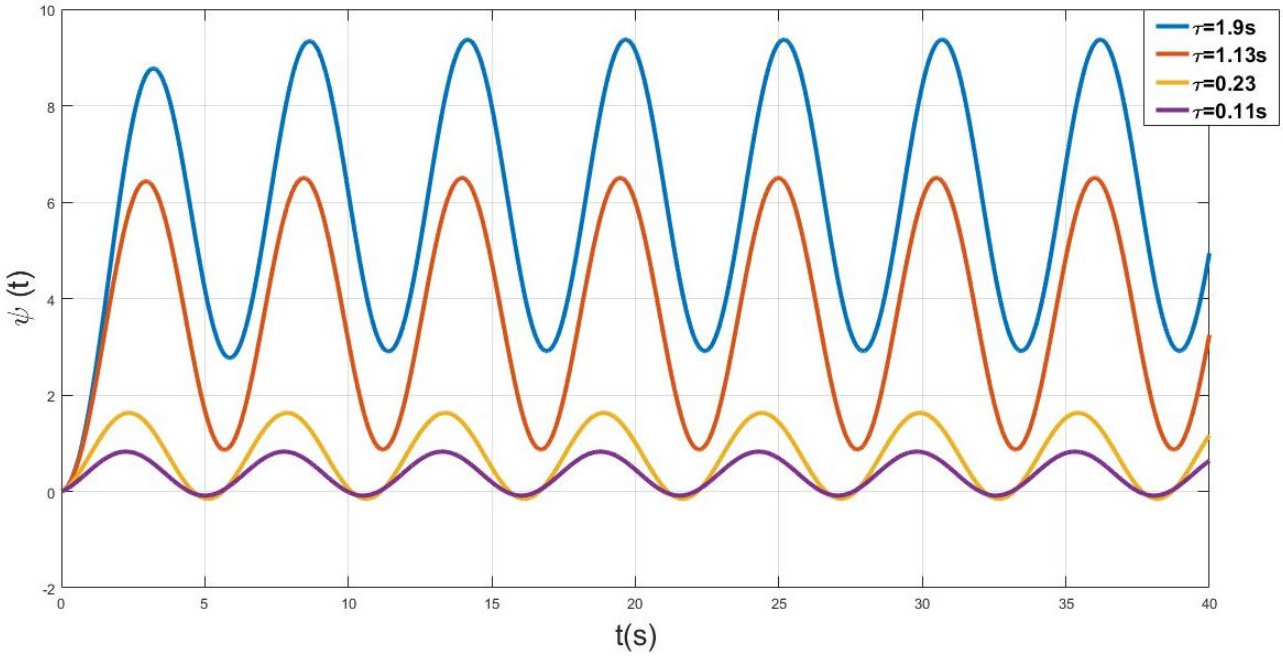

Figure 5.11: Yaw rotation responce to the precession axis input rotation.

Chapter 6

ISWEC components selection

6.1 Introduction

In the previous chapter all the analyses computed have been performed with the aim of the maximization of the gross power production for having hints about the general size of the device. A step forward is now required for the availability of a tool able to give a more quantitative results. Losses in this kind of application(power production device) play a key role: then a function able to choose the most suitable bearings for a given device size and configuration will be implemented on Matlab. The PTO will be selected considering the real characteristic curve of the electric power generators. The gear reduction parameter of the torque on the precession axis will be taken into account as well.

6.2 Bearing Power losses

Some specification about the flywheel bearings can be obtained at this level. These are crucial component in the overall system, since they are bearings, the highest mechanical loads in the system and great part of the mechanical losses are due to the resulting friction. The procedure for the designing radial and thrust bearings is described in this paragraph. First componets to be studied are the radial bearings. These consist of a couple of roller bearings sustainig the torque acting on the y_2-axis, $M_{E_{fw}}$ referred to the gyroscope structure and called T_λ.

6.2.1 Configuration

The bearings have to be choosen to support either the gyroscopic torques and the flywheel weight. In figure 6.1 is shown the gyroscopic group, in which are identified five bearings, two of which are inside the chamber(two identical radial roller bearings), and three outside it(two identical radial roller bearings and a spherical roller thrust bearing). The latter are subjected to a very low angular speed, and they are required to support the whole wheigh of gyroscopic structure, which may be directed both along the precession axis and the $x - axis$ according to the inclination of the structure. The overall load are relatively low, and therefore these bearing do not require any special maintenance. Instead, the bearings inside the chamber are more stressed for the very high load and for the achieved operating temperature.
The choosen bearings configuration is an optimal solution as long as the two bearings supporting the flywheel axis are radial spherical roller bearings capable to support an axial load due to the weight of flywheel when it oscillates according to the pitch motion of the hull.

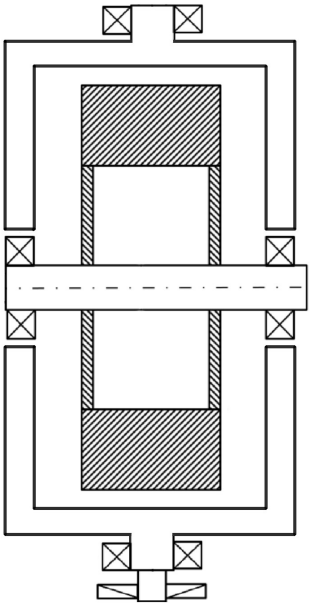

Figure 6.1: Bearings configuration scheme.

These bearings belong to the developed SKF Explorer performance class. An example

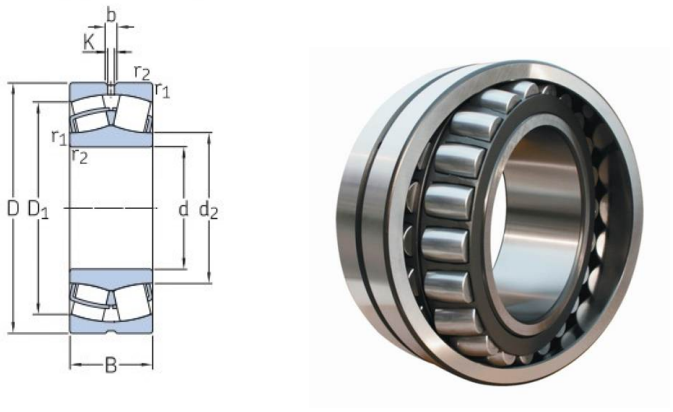

(a) *Bearing technical drawing* **(b)** *Bearing example.*

Figure 6.2: Spherical roller bearing configurations.

of bearings configurations for a specific inner diameter value d is shown in Tab.6.1. This kind of bearings have been choosen for the characteristic in term of performance:

- higher dynamic load carrying capacity compared to conventional design bearings;
- improved wear-resistance;
- reduced noise and vibration levels;
- less frictional heat;
- significantly extended bearing service life;

d (mm)	B(mm)	D(mm)	Series	$C_0(kN)$	C(kN)
190	52	260	239	800	414
190	75	290	230	1340	865
190	100	290	240	1800	1120
190	104	320	231	2080	1370
190	128	320	241	2500	1600
190	92	340	222	1700	1270
190	120	340	232	2400	1660
190	132	132	223	2650	2120

Table 6.1: Example of SKF bearings selection for a given inner diameter d

6.2.2 Model

It is now necessary to define all the parameters that are required to take into account for a correct bearing selection. It is then presented a computation which shows how the ISWEC operating condition defines a suitable bearing for every specific case. Here below is presented the expression of the torque which results from the interaction between the precesion axis and the flywheel axis. It generates a force which is entirely discharged on the bearings.

$$M_{E_{fw,y2}} = \vec{M_E} \cdot j_2 = I_{fw}\ddot{\lambda} - (J - I_{fw})\dot{\epsilon}\dot{\psi} - J\dot{\epsilon}\dot{\phi} \tag{6.1}$$

With the linearization around ϵ=0 and dropping the lower-magnitude terms, the next semplified relationship can be written:

$$T_\lambda = M_{E_{fw,y2}} = J\dot{\epsilon}\dot{\phi}+ \tag{6.2}$$

Dividing this torque for the distance between the component d_b, the radial force F_r is obtained:

$$F_r = \frac{T_\lambda}{d_b} \tag{6.3}$$

The bearings mounted on the flywheel axis have to support the weigth of component which can load the bearings both axially and along the radial direction depending on the hull oscillation δ. Then the radial force is described as follow:

$$F_r = \frac{T_\lambda}{d_b} + m_{fw}gcos\delta \tag{6.4}$$

The bearings are one of the most critical components in the system, so they are designed and choosen according to some duration specification. Input of this phase is the L_{10h} bearing life. In this pre-design phase the duration is computed with the constant load condition formula:

$$L_{10h} = \frac{10^6}{60\dot{\phi}_{nom}\frac{30}{\pi}} \left(\frac{C_b}{F_{b,eq}}\right)^{P_b} \tag{6.5}$$

where p_b is a bearing type dependent parameter, $\dot{\phi}_{nom}$ is the flywheel speed at the design wave state, C_b is the dynamic equivalent load coefficient and F_b is the radial force time

series which acts as load on the bearing. It corresponds to the previous defined F_r.
Once a defined load is acting on the bearing a corresponding flow of loss power, due to friction effects, is reported. As highlighted before such losses are a key point for a correct design of the device, then it' s required to estimate them as better as possible.

Losses caused by friction of the flywheel shaft bearings are modelled using the SKF catalogue method.The moment loss is defined as the the sum of four different term as shown in the equation below:

$$M_{loss} = M_{rr} + M_{sl} \tag{6.6}$$

where

- M_{rr} is the rolling frictional moment, and include effect of lubrificant starvation and inlet shear heation[Nmm]
- M_{sl} is the sliding frictional moment, and include effect of the quality of the lubrification condition[Nmm]

These two terms are then define as follow:

$$M_{rr} = G_{rr}(\nu n)^{0.6} \tag{6.7}$$

where

- G_{rr} is a variable which depends on the bearing series, the mean diameter and the radial and axial load. In partcular it is defined as follow:

$$G_{rr,e} = R_1 d_m^{1.85}(F_r + R_2 F_a)^{0.54} \tag{6.8}$$

$$G_{rr,l} = R_3 d_m^{2.3}(F_r + R_4 F_a)^{0.31} \tag{6.9}$$

$$G_{rr} = min(G_{rr,e}; G_{rr,l}) \tag{6.10}$$

- n is the rotationa speed [rpm].
- nu is the kinematic viscosity due to the lubricat [mm^2/s]

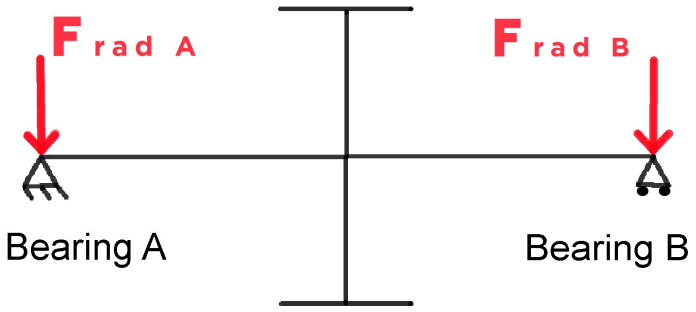

(a) *Flywheel axis on the horizontal direction.*

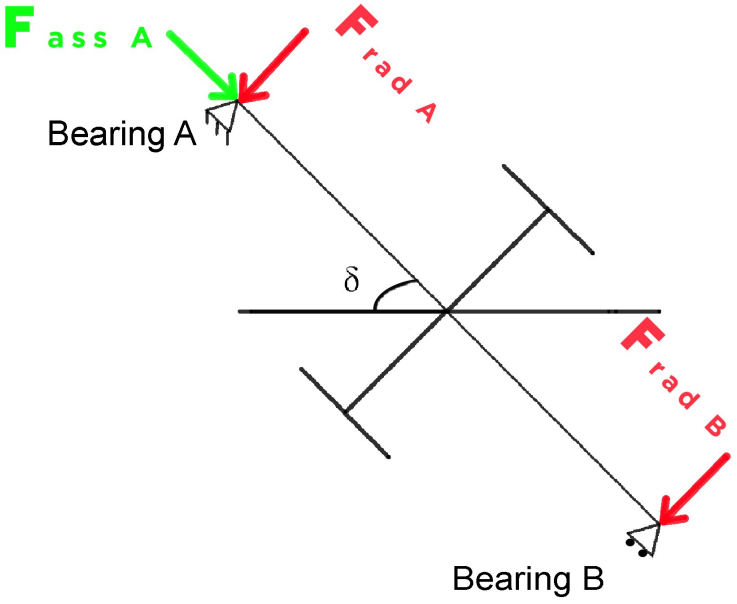

(b) *Flywheel axis rotate of the δ angle.*

Figure 6.3: Bearing load condition.

and then

$$M_{sl} = G_{sl}\nu_{sl} \tag{6.11}$$

where

- G_{rr} is a variable which depends on the bearing series, the mean diameter and the radial and axial load. In partcular it is defined as follow:

$$G_{sl,e} = S_1 d_m^{0.94}(F_r^4 + S_2 F_a^4)^{1/3} \tag{6.12}$$

$$G_{sl,l} = S_3 d_m^{0.94}(F_r^3 + S_4 F_a^3)^{1/3} \tag{6.13}$$

$$G_{sl} = min(G_{sl,e}; G_{sl,l}) \tag{6.14}$$

- nu_{sl} is the sliding friction coeffient specific for every bering series [mm^2/s]

The values S_1,S_2,S_3,S_4,R_1,R_2,R_3,R_4 are reported for the different bearing series in the SKF catalogue.

Bearing losses calculator-Matlab function A Matlab function $RadialBearingPowerLosses.m$ has been developed and implemented in the IDT for the automatic calculation of the power losses once the radial load is defined. The following parameters are set a priori in the function:

- A negligible value of the axial load is considered, F_a=0,1kN
- All the SKF-spherical roller bearing have been reported on Matlab building the 'n' data structure. In particular, a set of bearing which inner diameter ranging d_{min} and d_{max} has been considerd.

$$d_{min} \leq d \leq d_{max} \tag{6.15}$$

- the oil choosen for the bearing lubrification is the ISO VG 150.

The function input parameters depending on the working condition of the device are:

- The time series of the radial force F_r in N
- The flywheel angular velocini $\dot{\phi}$ in rpm

Then for any input set of parametrs the function is able to determine the power losses for each radial spherical roller bearing presented in the catalogue.

6.3 PTO configuration

The generator selected is the Siemens motor of the series 1FW32. It is a Permanent Magnet Synchronus Motor, a generic brushless which stator host the tri-phase windings and the rotor is an isotropic permanent magnet. In an induction motor during the regulation at costant power, it is possible to notice that an induction motor record a reduction of the maximum torque in the Field-weakening region. This phenomenon can be highlighted analyzing the characteristic curve.
The motor-specific limiting curves are used as basis when selecting a motor. These define the torque characteristic with respect to speed and take into account the motor limit based on the line supply voltage and the function of the infeed. The maximum motor torque, shown in Fig.6.4, is verified using the motor limiting curves. The following criteria must be taken into account when the motor is selected:

- The dynamic limits must be observed,this os, all speed-torque points of the load must lie below the relevant limiting curve;
- The thermal limit must be observed, that is, the RMS motor torque at the average motor speed resulting from the load duty cycle must lie below the S1 curve.
- In the case of synchronus motors, the maximum permissible motor torque is reduced at higher speeda as a result of the voltage limit curve. A clearance of 10% from the voltage limiting characteristic shoul also be observed to safeguard against voltage fluctuations.

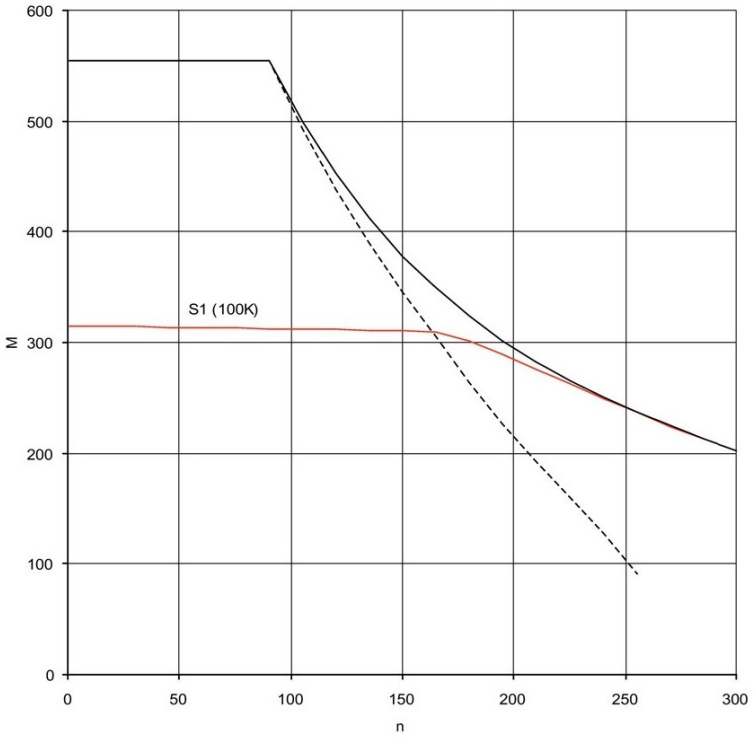

Figure 6.4: IDT logic scheme.

6.4 Bearings and PTO design tool

The updated version of the IDT receives as input the PTO specification, its characteristic curve and the value of the gear ratio for the torque reduction. Information about bearings are required, in particular the SKF catalogue has to be uploaded and the lower life limit that the final bearing has to respect is required. The news about the outputs, as specified in the scheme of Fig. 6.5, are about the productivity, because to the gross power are subtracted all the losses related to the selected bearing. Instead, considering the whole

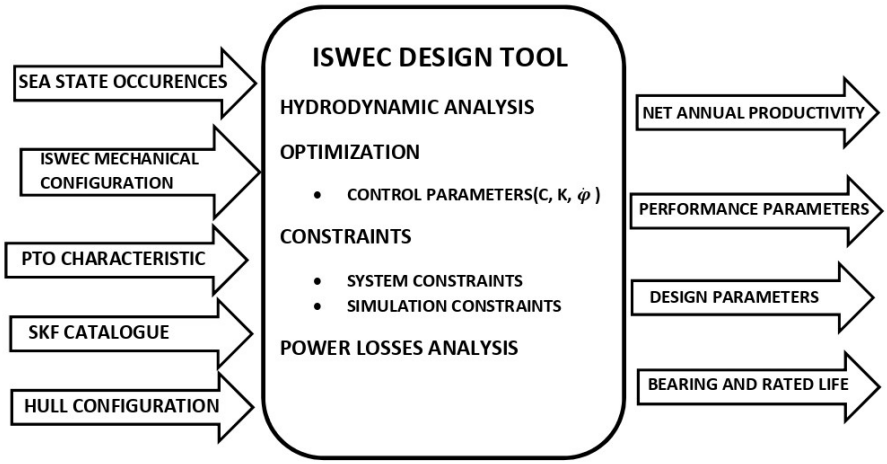

Figure 6.5: IDT logic scheme.

parameters involved in analysys the design flow follows the diagram represented in Fig.6.6.

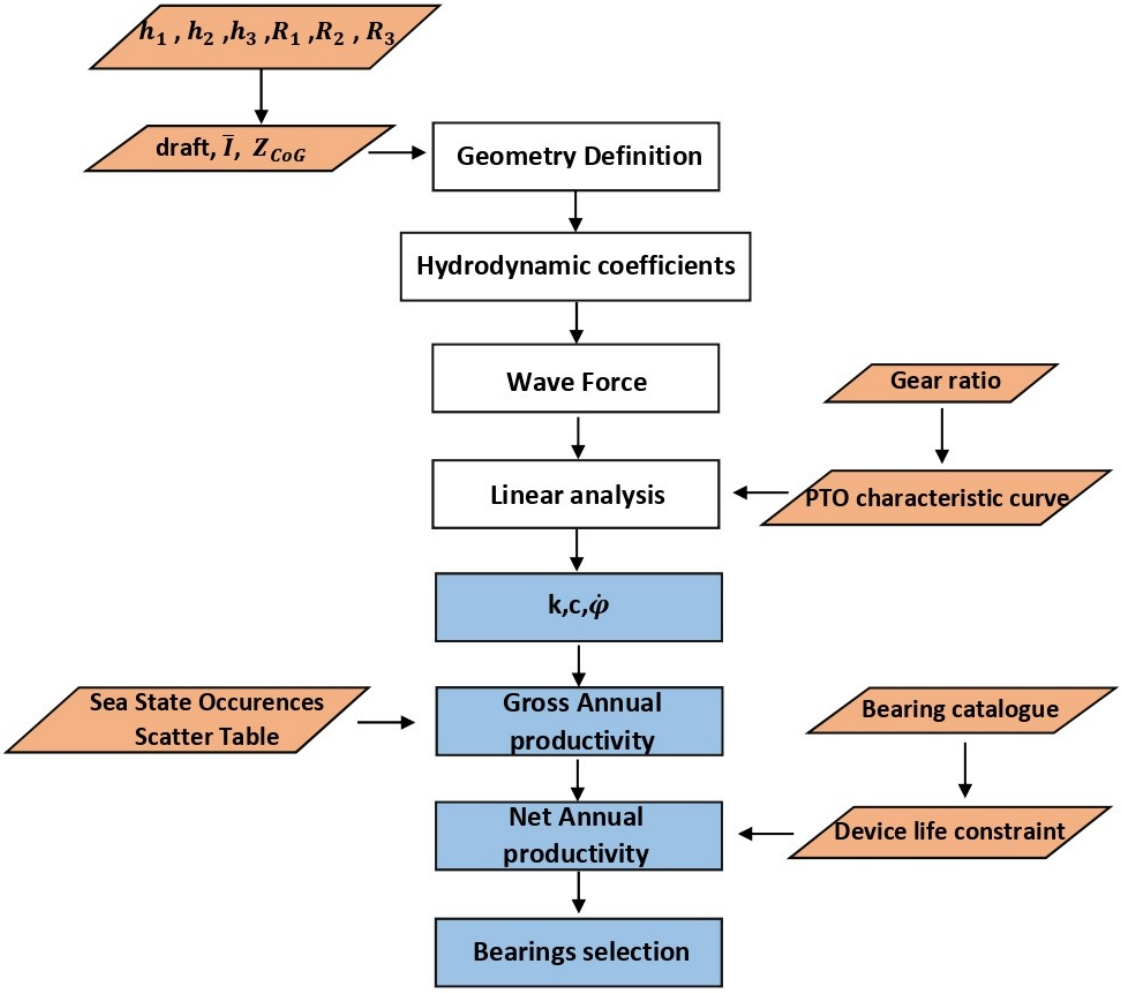

Figure 6.6: Design Process.

6.4.1 Bearing selection

The function input parameters depending on the working condition of the device are:

- The time series of the radial force F_r in N
- The flywheel angular velocini $\dot{\phi}$ in rpm
- Required bearing life in operating $hours$

Then for any input set of parametrs the function is able to determine the power losses for each radial spherical roller bearing presented in the catalogue keeping as constrain the following specification and conditions:

- Static failure condition:
  - The maximum load has to be lower then 1/4 of the static laod parameters(C_0) characteristic for each bearing.
- Fatigue failure condition:
  - For each wave(load) condition, the hour of expected operation at 95% confidence are :
$$L_{10h,i} = \frac{10^6}{60\dot{\phi}_{nom}\frac{30}{\pi}} \left(\frac{C_b}{F_{b,eq}} \right)^{P_b} \tag{6.16}$$
  - The overall life expectancy is a non linear combimation of different load condition:
$$L_{10h} = \frac{1}{\sum_{i=1} \frac{U_i}{L_{10h,i}}} \tag{6.17}$$
- Axial load capacty:
  - The maximum axial load that a radial spherical roller bearing can support is:
$$F_{ap} = 0.003Bd \tag{6.18}$$

    where
    F_{ap} is the maximum admissible axial load in kN B is the bearing width in mm;
    d is the bearing inner diameter in mm;

6.4.2 PTO selection

At this step the PTO saturation curve, as shown in Fig.6.7, is considered on Matlab implenting the followings piecewice function:

$$\begin{cases} F_{PTO} = -\frac{|\dot{\epsilon}|}{\dot{\epsilon}} F_{PTO}^{max}, & |F_{PTO}| \geq F_{PTO}^{max}; \\ F_{PTO} = -c_{PTO}\dot{\epsilon} - k_{PTO}\epsilon, & |F_{PTO}| < F_{PTO}^{max}; \end{cases} \tag{6.19}$$

Three PTOs have been elected and implemented in the system for checking their operating condition. Their properties are reported in Tab.6.2

ID	Code	Nominal Torque	Nominal speed	Maximum Torque	Maximum Speed	Conversion efficiency
-	-	[kN]	[rpm]	[kN]	[rpm]	-
1	1FW3281	2500	150	4050	1000	95
2	1FW3283	3500	150	5700	1000	95
3	1FW3285	5000	150	8150	1000	95

Table 6.2: Characteristic parameters of three selected PTO.

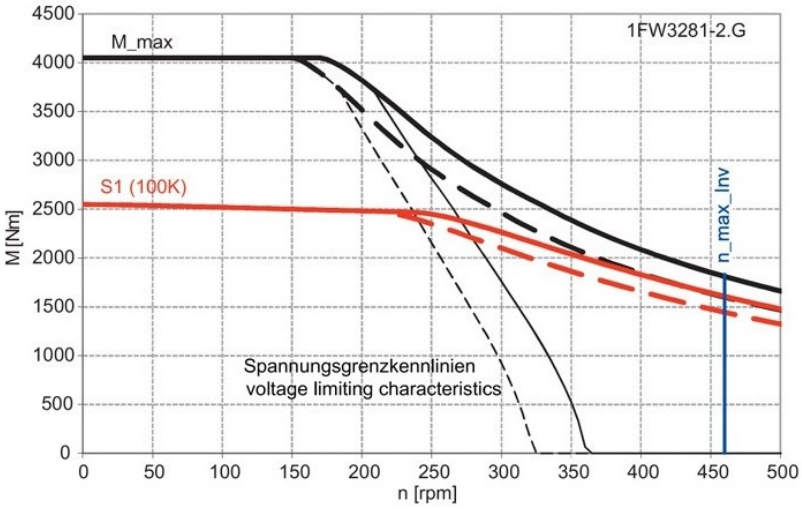

Figure 6.7: 1FW3281 characteristic curve.

6.5 Results

The productivity for each PTO, considering three different gear ratio have been evaluated and the results are represented in Figure 6.9. It is possible to notice that the productivity generally increases as the the PTO size increases as well. Considering that the precession axis in characterized by very high torque(order of magnitude of $10^5 kN$) and very low angular speed(about 20rpm), the gear ratio definition is very important in this case considering that the productivity is higher for bigger value of such parameter. The best

PTO Configuration	Gear Ratio	Gross Productivity	Losses	Net Productivivty
-	-	[MWh/year]	[MWh/year]	[MWh/year]
PTO ID:1	1	6.124	1.553	4.571
	5	9.354	2.174	7.182
	10	11.595	1.982	9.612
PTO ID:2	1	7.541	1.197	6.344
	5	10.809	2.044	8.765
	10	12.749	1.946	10.803
PTO ID: 3	1	7.2976	1.516	5.7814
	5	11.588	2.0142	9.574
	10	14.726	1.849	12.885

Table 6.3: Floater identification.

solution in term of productivity results for the PTO-3 considering a gear ratio of ten, but considering the size of the PTO as a discrimitation factor, the $PTO-2$ represents a good solution as well. The results relative to the $PTO-2$ is hereafter shown. The bering has the inner diameter of 90mm and gurantees a life of 34 years. All the design parameters matrix are plotted in Fig. 6.10 where is shown the variability of such parameters value during their operating conditions but at the same time constraints on the design parameters are respected.

d (mm)	B(mm)	D(mm)	Series	$C_0(kN)$	C(kN)
90	64	190	223E	695	610

Table 6.4: Example of SKF bearings selection for a given inner diameter d

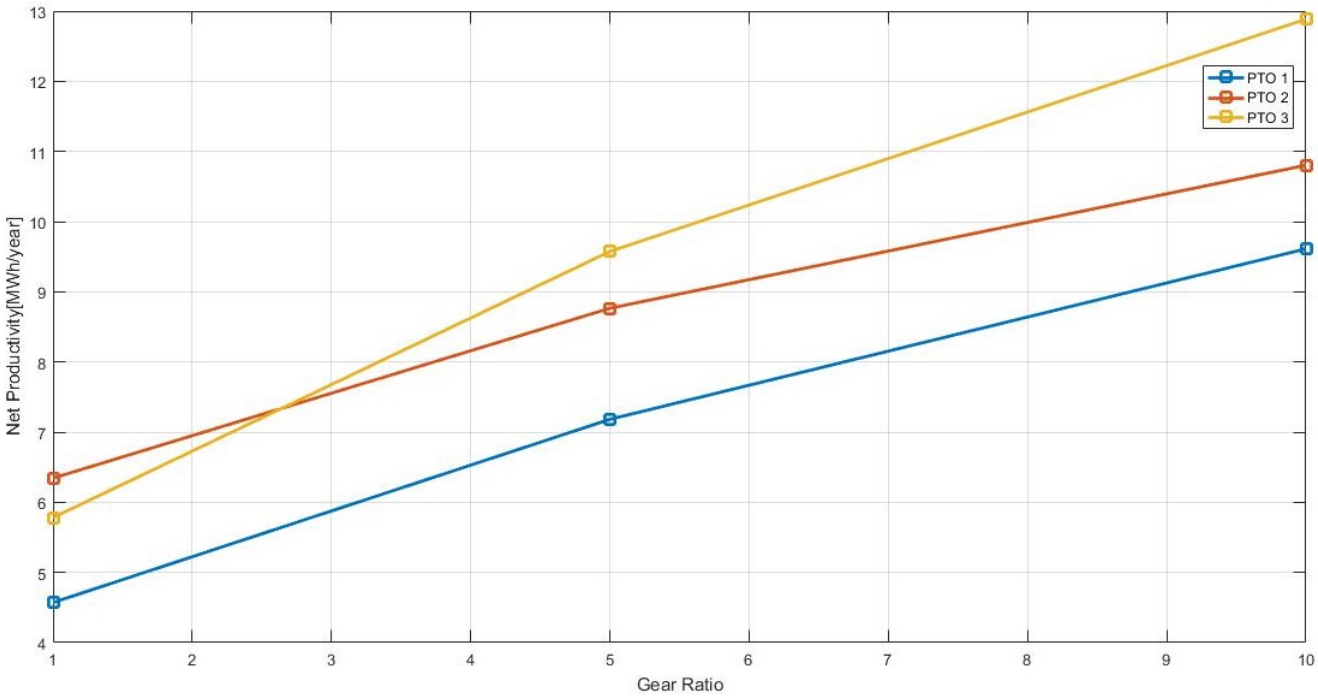

Figure 6.8: Net annual productivity.

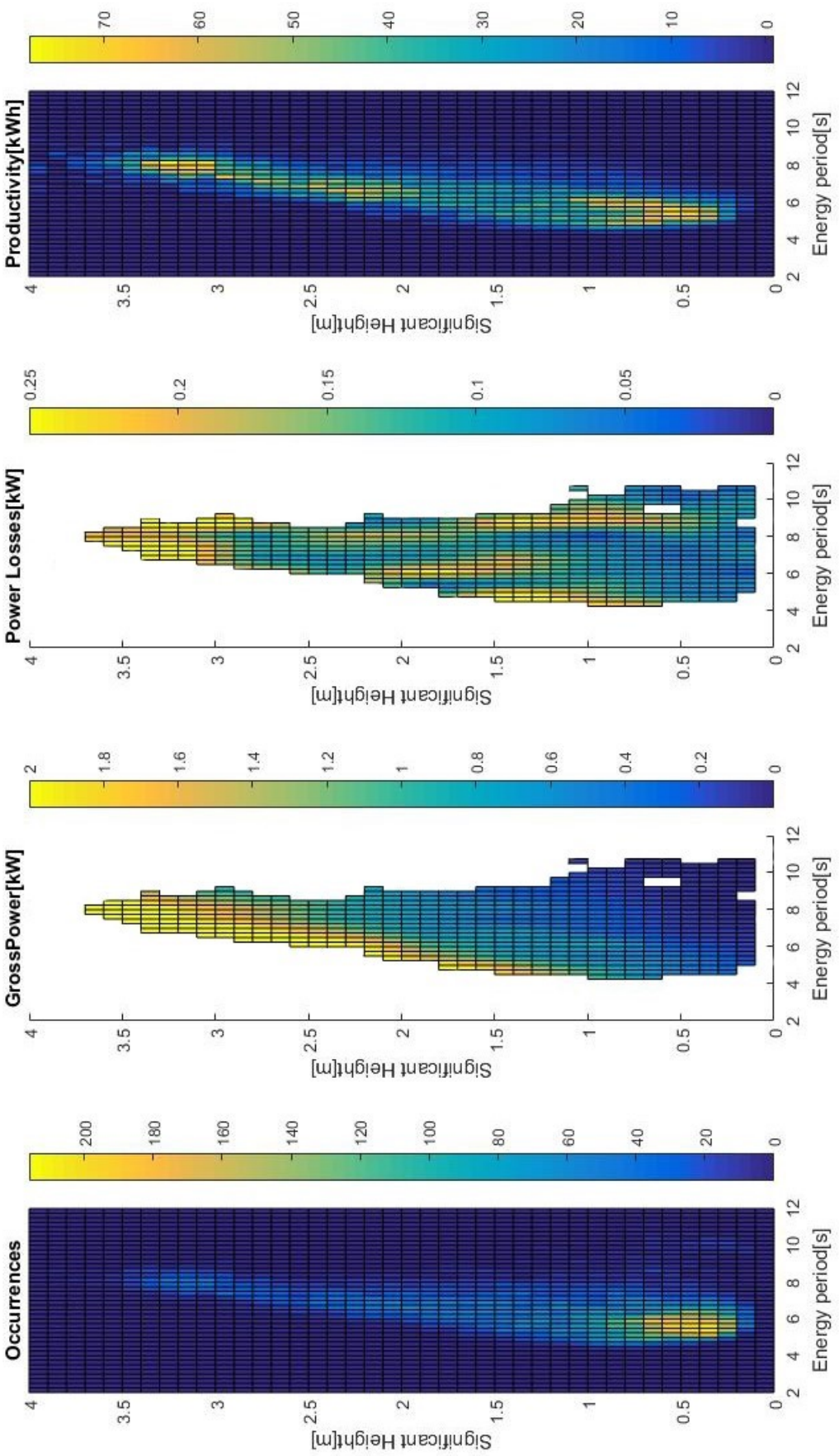

Figure 6.9: Net annual productivity.

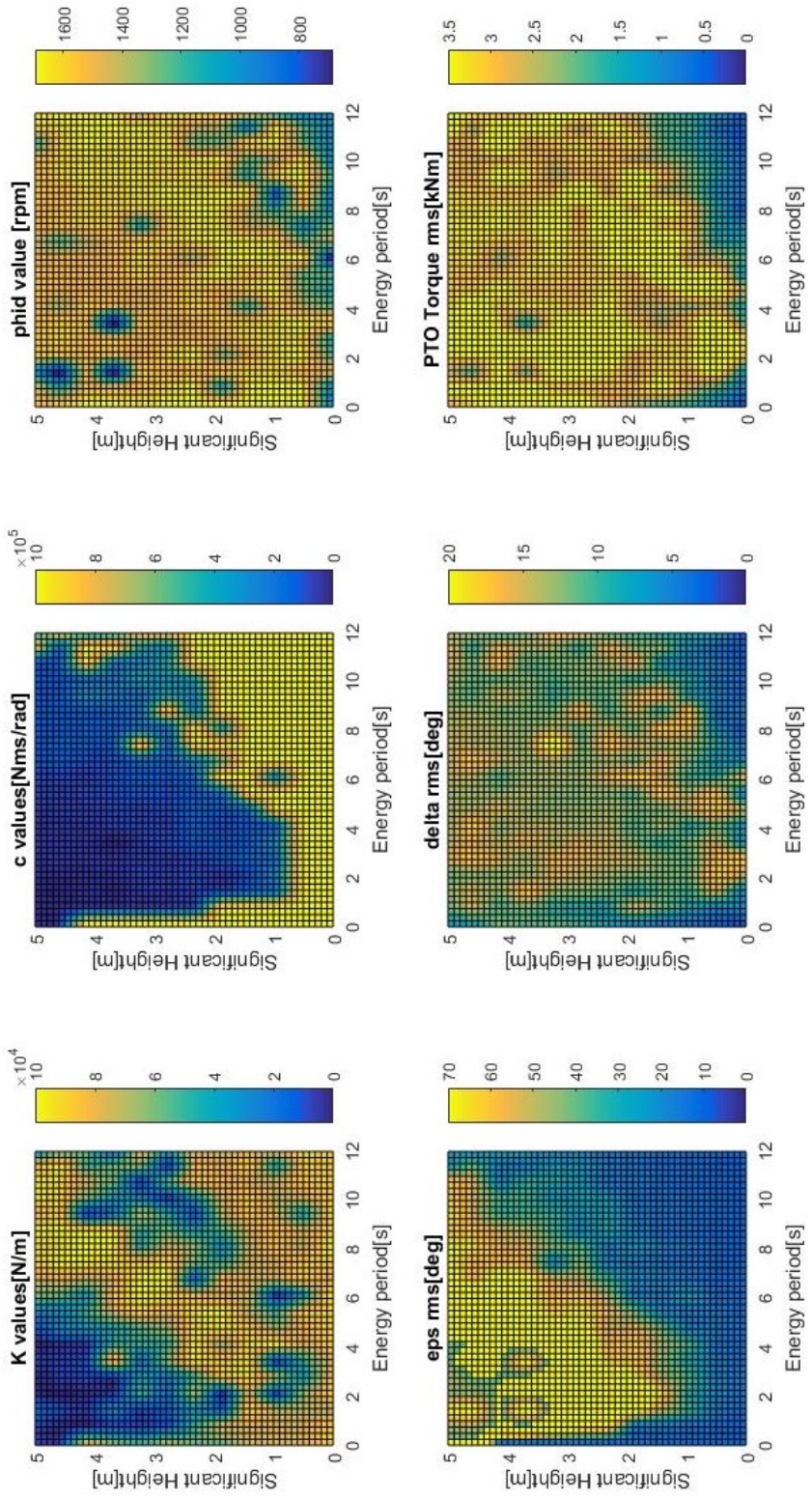

Figure 6.10: Design parameters and device performance results.

Conclusion

In this paper we deeply analyze and understand a new version of the omnidirectional-ISWEC device. The objective is to study the feasibility of this new solution that would represent a revolution in the WEC-technology space. Having as a starting point a new rotated reference system with the precession axis pointing towards the vertical direction, we have updated the ISWEC design tool ("IDT") and modified the underpinning equations. We have studied a new possible configuration of the hull, from a hydrodynamic perspective that, while having a more attenuate pitch response, grants a smoother manufacturing process and faster set-up. By deploying a local optimization algorithm, we have performed a comprehensive analysis of all the device components resulting in a new set of design parameters specific for each wave. As a result, for each different hull size fed to the tool, the MatLab code evaluates the resulting annual productivities taking into account the sea-state occurrences scatter table. Subsequently, we have analyzed the annual productivity sensitivity to the draft ratio parameters. Following our analysis, we took into account the losses by adding a new function able to find the bearing losses that maximize the net power production of the device. We then selected and simulated three different PTOs at different gear ratios, implementing their characteristic curves on the MatLab code. The final IDT provides as an output the design parameters, the selected bearings and the PTO size, for each given gyroscopic configuration. The final step of the analysis validates the hydrodynamic model of the IDT through a simulation program. We first performed a difraction analysis for the validation of the hydrodynamic parameters, namely added mass, radiation damping coefficient and Froude-Krylov coefficient. As a second and final step, we computed the relative error of the hull pitch response by comparing its root mean squares estimated in MatLab and Ansys time response environments. As a preliminary design, the described models neglect the non-linearities while adopting

a set of simplistic assumptions. However, we can state that we were able to establish a good starting point for the design process.
As a conclusion it is possible to state that such a project has a good potential in term of wave power exploitation. In particular, we have design a plant capable to produce up to 13kWh/year. We have seen and studied different plant considering the way different parameters influence the plant performance, such as the draft ratio, the gear ratio, the PTO size and bearings set up. While for the bearings selection the analysys performed is satisfactory, considering that the whole SKF catalogue is processed, for all the other parameters the analysys over a limited set of values has been performed. For the future design of the device is required to investigate a larger set of parameters, more hull configuration and include in the analysys the economic aspect which may be determinant in this kind of application for having the produced energy cost index. This kind of analysys is expected to have a great influence on the components selection, expecially on the PTO size. The following points are a list of improvments that can be adopted in order to have a more copmplete and precise analysis of a given device.

- **Complete model**: the IDT presented in this paper and all the analysis computed are made through a model which presents several simplifying hypothesis. In the next steps would be interesting to study the system considering the viscous damping term, the low frequency drift force and the mooring action term.

- **Simulink Validation**: the results given by the IDT are required to be validated through the non-linear model already implemented on Simulink. It will be then required to update the block diagrams to the new configuration and to eavluate the error of the resulting time series.

- **Yaw motion control**: as introduced in Chapter 5, the yaw motion of the hull would be a disturbing effect on the entire dynamic of the system. In this paper such effect has been just introduced, then it will be important to find a technological solution for controlling such responce of the structure.

- **Geometry definition**: only some floater modules combinations has been simulated and the final productivity has been evaluated. A step forward in this sense could

be the testing of all the possible combination for finding that one which maximize the productivity.

- **Optimization of the device**: the IDT can optimize the design parametrs through a global optimization algorithm. Next step is the design of tool a which can handle all the design parameters of the ISWEC (geometry of the hull, all the device losses, PTO selection, bearings selection) through a multi-objective optimization algorithm.

Bibliography

[1] Antonio F. O. Falcao, *Ocean Energies*, Workshop on Assessment of Potential and Promotion of New Generation of Renewable Technologies, 22 March 2011.

[2] B Drew, A R Plummer, M N Sahinkaya, *A review of wave energy converter technology*, University of Bath, UK, 16 June 2009.

[3] G. Genta, *Vibration Dynamics and Control*, Springer, 2009.

[4] Par Johannesson, Georg Lindgren, Igor Rychlik, Jesper Ryden and Eva Sjo, *WAFO-a Matlab toolbox for analysis of random wave loads*, Paper no. ISOPE 2000-GFC-02

[5] Markel Penalba, Thomas Kelly, John V. Ringwood *Using NEMOH for Modelling Wave Energy Converters: A Comparative Study with WAMIT*, 12th European Wave and Tidal Energy Conference, 2017.

[6] Sergej A Sirigu, Giacomo Vissio, Giovanni Bracco, Ermanno Giorcelli, Biaggio Passione, Mattia Raffero, Giuliana Mattiazzo. *Iswec design tool. Internation Journal of marine Energy*, 15:201-213,2016.

[7] Giacomo Vissio, *ISWEC torward the sea-Development, Optimization and Testing of the Device Control Architecture*. Ph.D thesis, Politecnico di Torino, 2017

[8] **Ansys**. *Ansys AQWA User Manual.*

[9] **SKF**:*Bearings Manual and Catalogue 2019.*

[10] **Siemens**:*SIMOTICS T-1FW3 complete torque motors*, Configuration Manual, Edition 11/2015